U. S. DEPARTMENT OF THE INTERIOR

U. S. GEOLOGICAL SURVEY

Tectonic evolution of the Crater Flat basin, Yucca Mountain region, Nevada

by

C. J. Fridrich

U. S. Geological Survey
Box 25046, Denver, CO

Open-File Report 98-33

Prepared in cooperation with the
U. S. Department of Energy Yucca Mountain Site Characterization Project

1998

ABSTRACT

Yucca Mountain is an arcuate, multiple-fault-block ridge on the rim of Crater Flat in southern Nevada. The ridge and alluvial flat are structurally linked and together constitute the Crater Flat structural basin. This late Cenozoic basin is located on the south flank of the southwest Nevada volcanic field, which in turn lies along the northeast margin of the Walker Lane belt, a northwest-trending zone of irregular topography and structure between the Sierra Nevada and the northern Basin and Range province. The Crater Flat basin is filled dominantly by the major ash-flow tuff sheets erupted from the central caldera complex of the volcanic field, at the north boundary of the basin. Relations in the volcanic rocks, including tilting, faulting, unit-thickness changes, and vertical-axis rotations, provide a detailed record of the tectonic history of Crater Flat and adjacent structural domains.

Strata within Crater Flat basin are tilted dominantly eastward to southeastward along a closely spaced system of mostly west- to northwest-dipping normal faults. This tilted-domino structural style resembles that of many areas of extreme extension and detachment faulting. However, in Crater Flat, as in much of the volcanic field, this style is developed at moderate to low percentages of extension, such that detachment faulting appears unlikely. Crater Flat formed by a combination of east-west to southeast-northwest extension and northwest-directed dextral deformation, the latter of which is indicated by oblique slickenlines on most intrabasin normal faults and paleomagnetic evidence of oroflexural bending along a northwest-trending axis through the basin. The spatial variation in the percentage of extension and in the degree of vertical-axis rotation within the Crater Flat domain resembles that of a triangular pull-apart basin. A major strike-slip fault(s) may be associated with this basin but, if so, it is somehow concealed. The caldera complex at the north boundary of Crater Flat influenced the structures of this basin by locally modifying the regional stress regime and by doming the rocks peripheral to the calderas; however, the structures of Crater Flat basin are products of regional tectonism, not of caldera collapse.

The new field evidence gathered in this study thus does not support previous suggestions that Crater Flat formed through the action of some single concealed master structure, such as a regional detachment fault, a caldera ring-fracture zone, or a major strike-slip fault. This is not to say that any of those three features are necessarily absent. Rather, the major conclusion at this point is that Crater Flat basin is a hybrid feature; its geometry reflects the combination of structural influences that are specific to its setting on the flank of a large caldera complex, at the boundary between the Walker Lane belt and the northern Basin-and-Range province, and at the periphery of a major domain - to the west - of extreme extension associated with detachment faulting.

In the Crater Flat region, belts of active extension have migrated, at times erratically, but with a regular west-stepping pattern during a major part of the late Cenozoic. In any one place, the evident tectonic pattern during the westward migration is abrupt onset of a pulse of rapid extension, followed by a progressive but slower decline in extension rate as the tectonic pulse migrated away. Scattered small domains, including a major part of the Crater Flat basin, have remained tectonically active at feeble rates long after passage of an extensional pulse.

INTRODUCTION

Investigations to evaluate Yucca Mountain as a potential site for a high-level radioactive waste repository have included geologic mapping of Yucca Mountain and adjacent areas, and are part of a broader, longer-term effort by the U. S. Geological Survey to characterize the geology and regional setting of the Nevada Test Site for the U. S. Department of Energy. Mapping efforts preceding the present study defined the basic structure and stratigraphy of the Yucca Mountain region, and provided the basis on which a number of alternative tectonic models were proposed (Christiansen and Lipman, 1965; Scott and Bonk, 1984; Maldonado, 1990; Maldonado and Hausback, 1990; Monsen and others, 1992; Minor and others, 1993; Wright and Troxel, 1993; Faulds and others, 1994; R. B. Scott, USGS, unpub. data). Important work supporting the geologic mapping effort includes geophysical investigations (Snyder and Carr, 1984; Rosenbaum and others, 1991; Grauch and others, 1993; Hudson and others, 1994), and geochronologic studies (Sawyer and others, 1994).

This paper decribes the results of 12 months of field work by the author from 1992 through 1996. This field work focused on collection of detailed map data in areas to the west of the proposed repository area, where no detailed mapping was previously available, and on field checking areas in which detailed mapping was completed by previous workers. The new field work includes complete remapping of two and a half 7.5-minute quadrangles (Fridrich and others, unpub. data). Because these new maps have not yet been published, they are cited below as - new field data, this study.

A major focus of the new mapping has been the documentation of angular unconformities, unit-thickness changes across faults, and kinematic indicators along faults. This new data is used, in conjunction with the preceding geologic and geophysical data: (1) to discriminate the structural domains and domain boundaries of the Yucca Mountain region, (2) to develop a comprehensive picture of the internal structure of the Crater Flat basin, the domain in which Yucca Mountain lies, (3) to define the late Cenozoic tectonic evolution of Crater Flat basin and adjacent domains, and (4) to evaluate the principal tectonic models that have been proposed for the Yucca Mountain area.

DEFINITION OF CRATER FLAT BASIN

The Yucca Mountain region is located in southern Nevada, in the southwest Great Basin (Figure 1). Yucca Mountain itself is an arcuate, multiple-fault-block ridge that extends around the north, east, and south flanks of the Crater Flat alluvial basin (Figure 2). This arcuate ridge and the "flat" it nearly encloses are structurally linked; together, they constitute a single domain in terms of their structural style and tectonic history, and they are distinct in these features from adjacent domains.

In terms of overall fault pattern, the Crater Flat/Yucca Mountain domain is a graben. This domain is bounded by an east-dipping range-front fault on the west side and the vast majority of faults within this domain are antithetic faults in the sense that they face into the range-front fault and are coeval with it (Figures 2 and 3). As discussed below, this domain apparently is also bounded by a major west-dipping normal fault on the east side (Figure 2). Thus, the Crater Flat/Yucca Mountain domain basically fits the definition of a structural basin, despite the uplifted ridge (Yucca Mountain) that occupies a major part of it. For simplicity, the Crater Flat/Yucca

Mountain domain is hereafter referred to as the Crater Flat basin.

The Crater Flat basin is one of numerous extensional basins of differing sizes, shapes, and structural styles that lie within the Walker Lane belt (Figure 1). Herein I apply Stewart's (1988) nongenetic definition of the Walker Lane belt as the 100-to-300-km wide by 700-km long northwest-trending zone of irregular topography and structure that intervenes between the Sierra Nevada and the northern Basin-and-Range Province. Whereas genetic interpretations of the Walker Lane belt are controversial, existing evidence is unequivocal that this belt contains numerous subregional-scale structures that are diverse expressions of small to moderate amounts of strike-slip deformation, within an overall regime of east-west to southeast-northwest extension (Figures 1 and 2). The oblique-slip and strike-slip faults within the Walker Lane belt are, for the most part, shorter and less continuous than is possible to show at the scale of location map (Figure 1), and the lack of thoroughgoing strike-slip structures is in fact a defining feature of this belt (Stewart, 1988).

The Crater Flat basin is defined here for the first time (and see Fridrich and others, 1998). The published alternative conceptions of the tectonic framework of the Yucca Mountain area are too numerous to review in detail, but they can be summarized in three end-member categories, according to the dominant process that is used to explain the major structural features of the Crater Flat/Yucca Mountain domain. According to one theory, Crater Flat formed as a caldera complex (Carr, 1982; Carr and Parrish, 1985; W. Carr and others, 1986; Carr, 1990). Another hypothesis is that Crater Flat is part of a rift that extends through the central part of the Amargosa Desert, to the south (Figure 2), and that is genetically related to the strike-slip faulting of the Walker Lane belt (Schweickert, 1989; Wright, 1989; Carr, 1990). The third end-member explains the structural features of Crater Flat and Yucca Mountain as being the result of detachment faulting (Hamilton, 1988; Scott, 1990).

Each of these three groups of theories has distinct implications that makes them at least partly testable. For example, the structures of calderas have geometries that reflect the fact that the deformation is dominantly vertically directed (tumescence, collapse, and resurgence; Smith and Bailey, 1968; Lipman, 1984). Once a subcaldera magma chamber solidifies, the caldera becomes a fossil structure; and the total life-cycle of a large ash-flow caldera system typically is on the order of hundreds of thousands of years. The rift hypothesis predicts that master strike-slip fault(s) are present at least at the ends of the rift, and perhaps as a continuous structure through the rift basin. All published versions of the detachment fault hypothesis infer that the postulated detachment fault under Crater Flat and Yucca Mountain was originally rooted to the west, and formed before the uplift of Bare Mountain severed the structural connection between Crater Flat and the highly extended Bullfrog Hills domain, on the north and west sides of Bare Mountain (Figure 2).

A common element in the three published end-member theories for the tectonics of Crater Flat basin is that they invoke a dominant controlling structural feature that is concealed. If unequivocal exposures of a caldera, a master strike-slip fault, or a detachment fault were present within Crater Flat basin, there would not be the latitude for the broad differences of opinion that exist on the tectonics of this area. In evaluating these theories, the approach taken here is not focussed on weighing the arguments for and against the presence of concealed master structures, but rather on developing an understanding the system based on observations of exposed features and from other ground-truth evidence, starting with the external and internal structure and the stratigraphy of the Crater Flat basin.

Physiographically, Yucca Mountain is formally defined as the arcuate ridge that encloses Crater Flat on all but the west side, as discussed above (Figure 2). In common usage, however, Yucca Mountain is usually taken as being only the north-trending part of the ridge that flanks the eastern side of the alluvial flat (Figure 3), and this convention is retained below.

VOLCANIC SETTING

Crater Flat basin lies on the south flank of the southwest Nevada volcanic field, which consists of a central cluster of overlapping and nested ash-flow calderas (Figures 2 and 3), surrounded by an extensive apron of outflow tuffs and lesser lavas and volcaniclastic sediments (Sawyer and others, 1994). From about 15.2 to 11.4 Ma, volcanism in the volcanic field was almost entirely silicic and was dominated by voluminous ash-flow eruptions (Table 1). Early cycles of volcanism built to a peak in eruptive volume rates between 12.8 and 11.4 Ma. Progressive decline in eruptive-volume rates since about 11.4 Ma has been accompanied by changes first to bimodal rhyolite-basalt volcanism from about 11.4 to 7.5 Ma, then to intermediate- to small-volume basaltic volcanism from about 7.5 to 2.5 Ma, and finally to very small volume basaltic volcanism in the Quaternary.

Seven major volcanic sequences were emplaced in the Yucca Mountain area before and during the evolution of the Crater Flat basin, and provide the major time-stratigraphic control for this study (Table 1). The sequences are: (1) the 14 Ma Lithic Ridge Tuff and related tuffs, lavas, and intrusions, (2) the formations of the 13.5 to 13.1 Ma Crater Flat Group - the Tram and Bullfrog Tuffs, and related lesser units, (3) the 12.9 Ma Calico Hills Formation (bedded tuffs and lavas), (4) the formations of the 12.8 to 12.7 Ma Paintbrush Group - mainly the Topopah Spring and Tiva Canyon Tuffs, (5) the 12.5 Ma Windy Wash Lavas and interfingering, related tuffs, (6) the 11.7 to 11.4 Ma Timber Mountain Group, which includes primarily the rhyolite of Fluorspar Canyon (tuffs and lavas) and the Rainier Mesa and Ammonia Tanks Tuffs, and (7) a group of basalts dated at 10.5 to 11.3 Ma. Of the above, the Crater Flat, Paintbrush, and Timber Mountain Groups are the principal bedrock sequences exposed in Crater Flat basin. Additional rock units that provide valuable local constraints on the tectonic evolution of this area include lanslide breccias, basalts, and ash-fall tuffs (Table 1).

The tectonic history that occurred during emplacement of these units is recorded by features such as stratigraphic burial of fault scarps and related stratal tilts, and abrupt thickness changes of units across faults. The best control on the structural evolution of the area is provided by the voluminous ash-flow tuffs because these widespread sheets buried much preexisting topography. The tops of the voluminous welded tuff sheets and the compaction foliations within them can be used as paleohorizontal indicators, with appropriate precautions (for example, recognition of primary tilting of compaction foliations induced by post-welding flow; Chapin and Lowell, 1979).

STRUCTURAL BOUNDARIES OF CRATER FLAT BASIN

The Yucca Mountain region consists of a mosaic of domains separated from one another by structural zones across which abrupt, fundamental changes are present in the style, timing, and magnitude of extension and other deformation (Figure 3).

The western boundary of the Crater Flat domain is the Bare Mountain range-front fault, which separates the ≥3-km-thick Tertiary basin fill of westernmost Crater Flat from the 1-km-high uplift of Paleozoic and latest Precambrian sedimentary and metasedimentary rocks of Bare Mountain (Snyder and Carr, 1984; Ackerman and others, 1988; Figure 3). At the north end of Bare Mountain, the range-front fault splits into three faults (Figure 3); two of these are different-age strands of the Tram Ridge fault, which is the northern extension of the Bare Mountain fault through Tertiary rocks, and the third is the Tate's Wash Fault, a northeast-striking high-angle normal fault system that separates the Bare Mountain uplift from the closely related Tram Ridge horst.

Bare Mountain and the Tram Ridge horst together constitute a septum of less-extended (from 14 Ma to present), relatively uplifted rocks separating Crater Flat basin from the highly extended Bullfrog Hills domain to the west. Despite the lesser extensional deformation within the Bare Mountain/Tram Ridge domain after 14 Ma, the Paleozoic rocks in this domain were strongly extended in a pre-Miocene tectonic event(s) that predated the formation of most and perhaps all of the domain boundaries discussed here, as well as the formation of the southwest Nevada volcanic field. Moreover, the Bare Mountain/Tram Ridge domain underwent extensive tectonic denudation related to the post-14 Ma extension that occurred around it, as discussed below.

To the north, the Crater Flat basin has a complex termination at the southern margin of the Timber Mountain caldera complex (Figure 3). One aspect of this domain boundary is a change in structural style from predominantly down-to-the-west faulting south of the margin of this caldera complex, within Crater Flat, to predominantly down-to-the-east faulting inboard of the caldera moat, within the fill of the 12.7-12.8 Ma Claim Canyon caldera. A second aspect is the truncation, by the 11.6 Ma Rainier Mesa and 11.45 Ma Ammonia Tanks calderas, of most of the extensional faults that postdate the 12.5 Ma rhyolite of Windy Wash. A third aspect is that faults younger than 11.45 Ma decrease in throw toward the north boundary of Crater Flat basin, and largely terminate near the margin of the caldera complex.

The northeast boundary of Crater Flat basin is Yucca wash (Figure 3), an alluvium-filled valley inferred to be underlain by a northwest-striking right-slip fault (Scott and Bonk, 1984; Scott, 1990). This fault is nowhere exposed; it is inferred because Yucca wash is a linear valley that separates Yucca Mountain from a domain to the northeast in which the 12.7-12.8 Ma Paintbrush Group and older rocks are more extended than they are on northern Yucca Mountain. The abrupt transition to greater faulting and tilting on the northeast side of the valley suggests the presence of a right-slip fault in the valley. Several small subparallel faults are exposed within about 5 km to the south of Yucca wash, on northern Yucca Mountain, and these exposed northwest-trending faults demonstrably are right-lateral strike-slip faults (Figure 3; Scott and Bonk, 1984). Whereas detailed mapping and geophysics have failed to demonstrate dip-slip offset across Yucca wash (W. Day, USGS, written comm., 1996), that evidence does not preclude the presence of a concealed strike-slip fault. Moreover, the abrupt large change in structural style across this linear valley indicates that it is a structural domain boundary despite that the nature of the concealed structural feature that forms the boundary is not firmly established.

The east limit of the Crater Flat basin is hidden under the Quaternary sediments of Jackass Flats, a shallow alluvial basin on the east side of Yucca Mountain (Figures 2 and 3). The closest exposures of bedrock to the east of Yucca Mountain are those of the Rock Valley domain.

Extension in the Crater Flat domain peaked between 12.7 and 11.6 Ma, and the structural pattern reflects dominant extension and lesser dextral shear, as discussed below. In contrast, field relations in the Rock Valley domain indicate two peaks in extension rate, one before and during deposition of Oligocene sedimentary rocks, and another after emplacement of basalt flows dated at about 10 Ma (D. O'Leary, USGS, written comm., 1996). The units of the 12.8-12.7 Ma Paintbrush Group and the 11.7-11.4 Ma Timber Mountain Group are strictly conformable in Rock Valley, indicating tectonic quiescence during the interval of peak deformation in the Crater Flat domain. The structural style in Rock Valley is dominated by two populations of faults, an east-northeast-striking set with gentle rakes, and a north-northeast-striking set with steep rakes. Strike-slip deformation apparently has predominated over extension in Rock Valley, and the sense of that deformation is sinistral rather than dextral.

The east boundary of Crater Flat basin against the Rock Valley domain probably is a large concealed down-to-the-west fault known as the Gravity fault (Winograd and Thordarson, 1975), which is interpreted based on large coincident north-trending gravity and aeromagnetic gradients near the western limit of exposures in the Rock Valley domain (Figure 2). Based on modelling of the geophysical data, the Gravity fault is a large-throw (> 1 km), dip-slip fault comparable in length to the Bare Mountain fault and roughly parallel to it, but with opposing dip. Both faults can be traced southward, by virtue of their gravity expressions (Blakely and others, in press) to intersections with the northwest-striking Pahrump-Stewart Valley and Furnace Creek fault systems, near the Nevada-California border (Figure 2). The Crater Flat basin is thus one of a series of contiguous basins that together constitute the central Amargosa trough, a large graben-like feature which is marked by a north-trending gravity low, and which has been referred to in discussions of the geology of this region by Wright (1989), who called it the Amargosa Desert rift zone and by Carr (1990), who included the caldera complex to the north in defining the Kawich-Greenwater rift.

The south boundary of the Crater Flat basin is concealed; hence, geophysics is the major available basis for deducing its location. The central Amargosa trough as defined here can be divided into three basins, which are separated by two narrow gravity highs (Blakely and others, in press). These small gravity highs within the trough appear to be roughly aligned along southwest and northwest projections, respectively, of the Rock Valley and Stewart-Pahrump Valley strike-slip fault systems into the central Amargosa trough (Figure 2). The southern boundary of the Crater Flat domain may thus be a structure related to the Rock Valley fault system.

An alternative hypothesis is that the eroded scarp that forms the southern limit of bedrock exposure in Crater Flat basin is a northwest-striking structure that has been called the Highway 95 fault (B. Slemmons, written comm., 1997). This hypothesis is supported by magnetic data, which show that the volcanic rocks of Crater Flat basin are abruptly truncated immediately south of this eroded scarp (Fridrich and others, 1996). Slemmons has proposed that the Highway 95 fault is a right-lateral strike-slip fault that extends northwestward of Crater Flat to form the scarp along the southwestern flank of Bare Mountain (Figures 2 and 3). As discussed below, additional work needs to be done to test this and other hypotheses that a number of large strike-slip faults may be present but largely concealed in the Crater Flat region.

INTERNAL STRUCTURE OF CRATER FLAT BASIN

As discussed above, Crater Flat basin has the overall form of a graben, with a large down-to-the-east range-front fault bounding the west side of the basin; a large, opposing, concealed fault on the east side; and a broad array of closely spaced, small-to-moderate-sized faults facing into, or angling into, the western range front across the majority of the basin (Figure 3). In the areas of bedrock exposure, only a narrow (0.5-to-2 km wide) zone along the westernmost edge of the basin is dominated by intrabasin faults that are synthetic to the range-front fault and by stratal dips westward into the range front. Exposed stratal dips in the rest of the basin with few exceptions are eastward or southeastward, which is consistent with the down-to-the-west (or -northwest) pattern of faulting that dominates in most of the basin (Figure 3).

Faulds and others (1994) suggest that the area of westward stratal dips in Crater Flat basin may be much more extensive than is apparent from bedrock exposures. Specifically, they propose that the area of total alluvial cover in the west-central part of the basin (Crater Flat physiographic feature; Figure 2) may lack bedrock exposure because it is the west-dipping flank of a structure they describe as an anticline, a broad rollover structure developed along the zone of maximum displacement on the Bare Mountain range-front fault.

The specific geometry Faulds and others propose cannot be tested definitively except by drilling. The general structural concept they propose, that the area of total alluvial cover (Crater Flat physiographic feature) is the area of maximum extension and subsidence in the Crater Flat domain, is consistent with existing geophysical and field data. Gravity and seismic refraction surveys indicate that the Crater Flat basin is deepest on the west side (Snyder and Carr, 1984; Ackermann and others, 1988), a conclusion which is supported by the general westward stratigraphic thickening observed in exposures of the late Tertiary volcanic rocks across the north and south parts of the basin (new field data, this study). The greatest localized thickening of volcanic basin fill, as well as the largest magnitudes of faulting and tilting in the basin, are exposed in the west half of the ridge that rims the southern margin of the Crater Flat physiographic feature (new field data, this study). Based on geometric considerations, the zone of maximum extension in the basin is not likely to be limited to the west half of this ridge; it probably extends on strike (north-south) for some distance, and probably includes much and perhaps all of the area of the alluvial flat to the north.

Normal faults within the Crater Flat basin have strikes that are northerly in the northeast part of the basin, changing to increasingly northeasterly strikes to the south and to the west across the basin (Figure 3). Another way to describe the fault pattern is to say that the faults within Crater Flat are roughly radial to the caldera complex to the north, and describe a curved pattern from north to south across the basin (Figure 3).

Paleomagnetic data indicate that the curved pattern of faulting down the east side of the basin (southward across Yucca Mountain) is due to southward-increasing clockwise rotation (Rosenbaum and others, 1991; Hudson and others, 1994). Preliminary paleomagnetic data collected in the northern part of Crater Flat suggest that the observed radial pattern of faulting around the caldera complex is partly a primary feature, but has been accentuated by westward-increasing clockwise rotation across the north part of the basin (M. Hudson, USGS, unpub. data). Thus the variation in the strikes of faults within Crater Flat basin largely reflects the pattern of vertical-axis rotation in the basin, but it also reflects localized modification of the regional stress field in the vicinity of the caldera complex at the north boundary of the basin, as suggested by Christiansen and others (1965) and Cummings (1968).

Within the Crater Flat basin, a northwest-trending "hinge-line" can be discriminated that separates an area of predominantly north-striking faults, to the northeast, from an area of predominantly northeast-striking faults, to the southwest (Figure 3). Fault strikes in the northern and southern parts of the basin are based on mapping (Scott and Bonk, 1984; R. B. Scott, USGS, unpub. data; new field data, this study), whereas in the central area which is largely covered by recent alluvium and Plio-Pleistocene basalts, existing field data (Faulds and others, 1994; Simonds and others, 1995) were augmented by aeromagnetic data. Abundant narrow linear aeromagnetic anomalies are present in this basin (Grauch and others, 1993); they principally reflect fault offsets of the highly magnetic Topopah Spring Tuff and allow tracing of major faults through many areas of alluvial cover (V. Langenheim, USGS, oral comm., 1995).

Based on paleomagnetic data, the hinge-line corresponds approximately to the contour of 20° clockwise rotation of the Tiva Canyon Tuff; greater than 20° dextral rotation is present to the southwest of this line and less to the northeast (Rosenbaum and others, 1991; Hudson and others, 1994; Fridrich and others, 1998). A subtle but abrupt topographic decline (lower on the southwest side) is present along most the the length of the hinge-line, reflecting a southwestward increase in the magnitude of extension. Most of the faults that cross the hinge-line show a pronounced southward increase in both Quaternary displacement and total bedrock displacement across it (Scott and Bonk, 1984; Menges and others, 1994; A. Ramelli, Nevada Bureau of Mines and Geology (NBMG), oral comm., 1995).

The above-described field relations suggest that the hinge line is a distinct boundary separating a less extended and rotated area to the east from a more deformed area to the west. The paleomagnetic data actually show a step increase in rotation to the west across the hinge-line in the northern part of the basin, but are only permissive of a smaller step change to the south. The zone of strong rotational deformation extends to the Bare Mountain range front; and the Bare Mountain/Tram Ridge domain has not been significantly rotated since 11.6 Ma based on existing paleomagnetic data (Hudson and others, 1994; M. Hudson, USGS, written comm., 1995). The area between the hinge-line and the Bare Mountain range front constitutes a transtensional structural zone, and is the area of greatest extensional and strike-slip deformation in the basin.

Nearly all of the normal faults in the Crater Flat basin show at least a small component of oblique offset. Most of the north- to northeast-striking intrabasin normal faults show a component of left slip. Left slip on these faults is consistent with the clockwise rotation of the blocks between the faults, as documented with the paleomagnetic data, and, from that perspective, is indicative of dextral shear throughout most of the Crater Flat basin. Given the late Cenozoic stress regime of the Great Basin, with the least principal stress oriented west-northwesterly, on average, the resolved sense of strike-slip shear on north-striking normal faults is right lateral (Figure 4A). However, when the blocks between the faults are rotating clockwise in response to this dextral shear stress, the horizontal component of movement on the normal faults then has the opposite shear sense (left-lateral), reflecting dynamic shear (slip that accommodates rotation; Figure 4B), rather than the static sense of shear.

Near the southernmost exposure of the Bare Mountain front, the strike of the range-front fault changes slightly, from north to north-northwest. Whereas the fault trace is concealed in this location, sheared surfaces are abundant in the quartzites that border the alluvium-covered fault trace. Many of these sheared surfaces have slickenlines with moderate-angle rakes and Riedel shears indicating that offsets were right-oblique and normal. Given the middle-to-late Miocene geometry of this domain boundary, with extensional faults of the Crater Flat basin oblique to the range front (Figure 3), some lateral offset on the range-front fault is required geometrically, at least in the Miocene. This geometric requirement could be filled by a minor component of horizontal offset on the southern part of the Bare Mountain fault, which is consistent with the field evidence. Several small exposures of the Bare Mountain fault are present, scattered along the length of the range front; and slickenlines on the fault plane indicate that it is high-angle fault with almost purely dip-slip offset in most of these exposures.

Whereas some of the structures that form the boundaries of the Crater Flat structural domain may have a strike-slip or oblique-slip character, as discussed above, no significant strike-slip faults have been observed within this domain by this author or any previous workers. The few strike-slip faults that have been mapped within the basin have horizontal offsets of <30 m and lengths of <5 km (Scott and Bonk, 1984; Day and others, in press). The larger examples of these minor strike-slip faults are strongly concentrated in the northeast and northwest parts of the basin.

At least two major internal faults within the Crater Flat basin are scissors faults; that is, they are normal faults that decrease in throw to a fulcrum point, past which they have the same approximate strike and dip, but are then reverse faults (Figure 3; Scott and Bonk, 1984; new map data, this study). Scissors faulting is easily conceptualized in the context of a basin in which blocks between faults have undergone varying degrees of vertical-axis rotation. If one fault block has experienced more rotation than the neighboring block, then that differential rotation will be expressed by an along-strike change in the magnitude of displacement of the fault that separates the two blocks and, in extreme cases, by a change from normal to reverse displacement.

A number of additional internal features of Crater Flat provide important evidence of the structural regime of this basin. For example, several broad folds (wavelengths in kilometers; amplitudes in 10's to 100's of meters) are present in the basin with axes that trend westerly to northwesterly, thus at high angles to the strikes of the major intrabasin faults. Faulds and others (1994) explained these folds as being due to along-strike changes in the magnitude of displacements on major intrabasin faults. Some of the folding within about 10 km of the Timber Mountain caldera complex may be related to the dynamics of the magmatic system as much or more than to regional tectonic forces, as discussed below.

Abundant short-wavelength folds in Crater Flat basin have axes that parallel the strikes of intrabasin faults; these folds dominantly are monoclines with their axes centered on the fault zones. The major intrabasin faults generally consist of a number of strands spaced out across zones as much as 0.5 km wide. These complex fault zones may break monoclines because the mapped structural complexity may not extend to depth, and the shallow rocks -the tuffs - may therefore be draped over larger, simpler (aggregate) fault offsets in the underlying Paleozoic rocks. These tight monoclines probably formed largely during the initial formation of the major faults and they are evidently brittle (rather than ductile) folds; the bending appears to be accommodated by the aggregate effect of abundant small dislocations along the cooling joints that riddle the tuffs, rather than by true plastic deformation.

TECTONIC HISTORY OF CRATER FLAT AND ADJACENT DOMAINS

The above synthesis of the external and internal structure of the Crater Flat domain provides a critical basis for testing alternative tectonic models for this area. An equally important element that is missing above is the element of time. The evolution of Crater Flat basin can be divided into three major phases: (1) events preceding development of Crater Flat basin as defined above (pre-12.7 Ma), (2) events involving the creation of this structural basin between 12.7 and 11.6 Ma, and extending to the end of the major period of tectonism in the basin at about 10 Ma, and (3) the waning cycle of tectonic activity in this structural basin, from about 10 Ma to the present. The following discussion addresses these three major phases of evolution, but follows stratigraphic or geographic divisions, reflecting the limitations of the field evidence.

Analysis of the Structure of Bare Mountain: Evidence for tectonic events that predate the southwest Nevada volcanic field

The Paleozoic and latest Precambrian sedimentary and metasedimentary rocks of Bare Mountain, on the west rim of Crater Flat basin, are strongly deformed (Figure 5). This deformation includes Mesozoic compressional structures (Monsen and others, 1992); however, an equal or greater component of the deformation is extensional, and is largely Tertiary. The Tertiary extensional deformation within Bare Mountain predates the major ash-flow tuff sheets of the southwest Nevada volcanic field because the structures associated with this extension are truncated at the boundaries of the range; they do not extend into the bordering 15-to-10-Ma volcanic rocks.

Unraveling the history of deformation of Bare Mountain is an uncertain exercise because: (1) The structure of this mountain is the result of a complex overprinting of multiple Mesozoic and Tertiary events, (2) few post-Paleozoic rocks are present within the uplift to constrain the timing and to distinguish the effects of separate Mesozoic and Cenozoic events, and (3) existing geologic mapping (Monsen and others, 1992) and petrologic studies (Hoisch and others, 1997) were not specifically addressed at developing field constraints on the relative ages of the structures within this mountain. The generalized map of the structures of Bare Mountain (Figure 5) inevitably reflects the author's preconceived notions with respect to how these faults should be grouped, as well as the apparent age relations between them; in contrast, the raw map data (Monsen and others, 1992) leaves abundant latitude for developing alternative interpretations.

The largest extensional structure within Bare Mountain is partly coincident with a large metamorphic-grade discordance that suggests several kilometers of uplift of a high-grade block on the west side of the mountain with respect to the rocks in the rest of the mountain (Figure 5). Hoisch and others (1997) ascribed this sharp discordance to a single structure which he named the Gold Ace fault. However, Monsen and others (1992) mapped the same contact as two contiguous faults that strike roughly perpendicular to one another, a north-dipping western fault, which they called the Coñejo Canyon fault, and an east-dipping eastern fault, for which Hoisch's name, Gold Ace, was used (Figure 5). Both faults place younger, more steeply tilted, lower metamorphic-grade rocks on older, more gently tilted, higher-grade rocks (Hoisch, and other, 1997). Whereas the Coñejo Canyon fault is a broad plexus of fault strands with a geometry similar to a duplex fault zone, the Gold Ace fault is mapped as being narrow and nearly planar (Figure 5).

If the Coñejo Canyon and Gold Ace faults constitute a single structure, as Hoisch proposes, then the right-angle bend that joins them must be a megascale mullion because this bend cuts across structure as defined by stratal attitudes in the surrounding rocks (Figure 5). The northeast trend of this putative mullion is inconsistent with the top-to-the-northwest transport that Hoisch proposes occurred on this fault. Monsen and others (1992) inferred, however, that the Gold Ace fault extends northward of the intersection with the Coñejo Canyon fault (Figure 5). This latter interpretation is supported by detailed surface and subsurface mapping by mining company geologists in this area (J. Greybeck, Cordex Exploration, oral comm., 1996), who have shown that the northward projection of the Gold Ace fault separates folded marbles to the west, from little recrystallized and virtually unfolded limestones to the east.

The planar Gold Ace fault appears to be a detachment structure because the rocks in the upper plate of this very large throw, low-angle fault are significantly more extended than are those in the lower plate, as evidenced by greater faulting and tilting in the upper plate (Figure 5; Monsen and others, 1992). This extension occurred dominantly along a system of northeast-striking low-angle (20 to 40°) normal faults that are confined to the upper plate and that have down-dip bedding offsets ranging from about 1 to 3 km apiece.

The difference in average stratal dips between the upper and lower plates of the Gold Ace fault could be explained by about 30° of tilting to the north-northwest, of the upper plate rocks, on average, relative to the lower plate rocks. This inferred structural tilting is roughly opposed to the dip direction of the northeast-striking faults. If the apparent tilting is subtracted to restore the upper plate rocks to a preextensional geometry, then the northeast-striking faults were high-angle (50 to 70°) faults when they formed. This last supposition is somewhat clouded by the possibility of significant later tilting during uplift of Bare Mountain. Nonetheless, the northeast-striking faults and the tilting of the upper plate rocks may thus be related as products of a single extensional event that resulted in a tilted-domino structural style in the upper plate of the coeval Gold Ace detachment fault.

In contrast to the Gold Ace fault, the Coñejo Canyon fault system is crudely planar at best, and appears to be weakly folded. In addition, the rocks cut by this fault system have numerous tight folds, many of which have geometries that suggest they may be drag features related to top-to-the-south movement along the Coñejo Canyon fault system. If so, this fault system is a Mesozoic thrust fault rather than a Tertiary detachment fault. The younger-on-older nature of this fault is not incompatible with its being a thrust fault because the rocks may have been thrusted before. In any case, the Coñejo Canyon fault is truncated by the Gold Ace fault (Figure 5) and is therefore an older structure.

The oldest generation of exposed faults in Bare Mountain Field are north-striking with dominantly high-angle dips to the east (Figure 5). These faults are truncated by the Gold Ace fault and most if not all of the thrust faults of Bare Mountain, including the Coñejo Canyon fault system, and are unlikely to be secondary structures related to these major low-angle faults because they are present in both their upper and lower plates. Although the north-striking high-angle normal faults may have moved during several different tectonic episodes, the fact that they are cut by thrust faults suggest that they formed before or during the Mesozoic era.

The major faults that bound the north and east sides of Bare Mountain provide absolute time constraints on the structural evolution of this uplift because activity on these faults is reflected in their field relations with the neighboring Tertiary rocks, as discussed below. The northern and eastern range-bounding faults appear to truncate most of the internal structures of Bare Mountain (Figure 5), as discussed above, suggesting that these internal structures predate the uplift of this range largely if not entirely. As discussed below, both the nature and the age of the steep, nearly linear scarp that forms the southwest boundary of Bare Mountain are, at present, poorly constrained.

The Bare Mountain fault forms the east boundary of the uplift, and appears to be a classic high-angle range-front fault. The Fluorspar Canyon fault forms most of the north boundary of Bare Mountain against the Tertiary volcanic rocks of the Bullfrog Hills domain (Figures 5 and 6). This structure is a detachment fault that apparently headwalls in a large low-angle breakaway scarp that forms the western boundary of the Tram Ridge horst, about 2 km west of the northeast tip of Bare Mountain (Figures 5 and 6). Assuming that the eastern part of the detachment fault strikes northerly and dips to the west in the plane of the exposed breakaway scarp, the Fluorspar Canyon detachment has a southern termination in the subsurface against the Tate's wash fault, the high-angle fault that separates the Tram Ridge horst from the Bare Mountain uplift. However, the Tate's wash fault decreases in dip to the west, and probably merges with the detachment fault about 2 kilometers southwest of the breakaway scarp. The western part of the Fluorspar Canyon fault, along the northwest border of Bare Mountain, dips to the north at angles ranging from 20 to 40° (new field data, this study).

Both the Fluorspar Canyon detachment fault and the Bare Mountain range-front fault evidently formed in the interval between 12.7 and 11.6 Ma. Significant downthrown thickening is present across the breakaway scarp of the Fluorspar Canyon fault and across the Bare Mountain-Tram Ridge fault (at the northeast corner of Bare Mountain; Figures 5 and 6) in all volcanic units that are 11.7 Ma and younger, and that are present and exposed in the vicinity of these faults. In contrast, thickness variations in units that are 12.7 Ma and older in the vicinity of these faults can largely be explained as resulting from the formation and burial of volcanic landforms (new field data, this study). Moreover, the ~15-to-12.7 Ma volcanic section is well exposed immediately adjacent to Bare Mountain along the north boundary of the uplift, and this section does not include any Paleozoic clasts or intercalated coarse sediments or breccias, as might be shed from a nearby uplift. The only intercalated sedimentary rocks observed in this section are planar-bedded fine-grained marls and tuffaceous sandstones. Most of these sediments appear to have been deposited in a lake or lake-shore environment; both petrified wood and fish bones have been observed in these rocks.

The uplift of Bare Mountain was accompanied by large-scale landsliding to the north and east. Rock-avalanche breccias are intercalated between the 12.7 Ma Tiva Canyon Tuff and the 11.7 Ma rhyolite of Fluorspar Canyon in the western part of Crater Flat, in the subsurface (Carr and Parrish, 1985), and on the surface in the eastern part of the Bullfrog Hills domain, on the north flank of Bare Mountain (new field data, this study). These breccias are proximal deposits composed of clasts of Paleozoic carbonates and the oldest Tertiary (14-to->15 Ma) sedimentary rocks; the ≤14-Ma volcanic rocks are absent; the best exposed deposits demonstrably thicken and coarsen toward the range, indicating that Bare Mountain is the source of these breccias. Although it cannot be proven from existing evidence that the Bare Mountain uplift did not exist before 12.7 Ma, the evidence indicates that the major uplift event of this range occurred between 12.7 and 11.6 Ma, and that the range was uplifted along the faults that currently bound the range on the north and east sides.

14+ to 13.1 Ma:

Within Crater Flat and the adjacent domains that are dominated by volcanic rocks, sufficient time-stratigraphic constraints are present to allow a chronologic treatment of the tectonic evolution. The earliest definable tectonism within the Crater Flat basin was underway at least by 14 Ma and is notable principally for its strong contrast in structural style with the tectonism that occurred in this basin after 13.1 Ma. Owing to the fragmentary exposure of volcanic rocks older than 13.1 Ma (Figure 7), the clearest evidence on the timing and style of this episode of tectonism in Crater Flat is derived from subsurface data.

Fridrich and others (1994a) used a combination of gravity data and subsurface control to infer that a buried graben is present under the northeast part of Crater Flat basin (Figure 7). The gravity data shows a narrow, northeast-trending trough-like low of about 10 milligals over northern Yucca Mountain (Snyder and Carr, 1984; Fridrich and others, 1994a) . This data was modeled by Oliver (USGS, oral comm., 1991), who estimated that the low results from a localized depression of the Paleozoic-Tertiary contact of about 500 m relative to the surroundings. The gravity low is interpreted as a graben, rather than as a paleocanyon, because the stratigraphic thickening into the low is a step change; six drill holes within the low all encountered 13.1-to-14 Ma volcanic sections of approximately the same thickness, and that thickness is about twice that of the equivalent strata in deep drill holes immediately to the north and south of the low (Fridrich and others, 1994a; Figure 7).

Tuffs emplaced between 14 and 13.5 Ma thicken strongly into the low (Figure 7), indicating that this was the period of major activity on the bounding faults. No change in stratigraphic thickness into the low is found in formations younger than the 13.1 Ma Prow Pass Tuff; hence, the graben evidently became inactive sometime between 13.5 and 13.1 Ma, and was then buried. The gravity low and, by inference, the buried graben under northern Yucca Mountain abruptly terminates in the vicinity of Yucca wash, suggesting that the inferred northwest-striking fault under Yucca wash was active in the same time interval as the buried graben.

East-northeast-striking faults that may be part of the same structural regime as the buried graben described above have been mapped in exposures of the 13.5-13.1 Crater Flat Tuff sequence in northwest Crater Flat and at the south end of Yucca Mountain (Figure 7; new field data, this study). In northwest Crater Flat, lavas and related bedded tuffs of the 13.35 Ma rhyolite of Prospector's Pass appear to be cut by two generations of faults, one of which cuts across the other, resulting in a checkerboard-like fault pattern. The north-to-northeast-striking fault set formed shortly after 12.7 Ma, based on constraints discussed below, whereas the east-northeast-striking faults appear to cut the 13.35 Ma rhyolite of Prospector's Pass and older rocks, but not the 13.25 Ma Bullfrog Tuff.

At the south end of Yucca Mountain, a single east-northeast-striking fault was mapped that cuts the 13.25 Ma Bullfrog Tuff, forming a fault scarp which was buried by the overlying 13.1 Ma Prow Pass Tuff (new field data, this study). The more easterly strikes of the pre-13 Ma faults in southern and northwestern Crater Flat relative to the trend of the buried graben of the same age in northeastern Crater Flat (Figure 7) is consistent with the spatial variation in vertical-axis rotation that occurred in this basin after 12.7 Ma (Rosenbaum and others, 1991; Hudson and others, 1994); all of these structures were roughly parallel before the post-12.7 Ma rotation.

Overall, the extensional deformation that occurred from 13 to ≥14 Ma within Crater Flat basin is minor relative to the deformation that occurred both before and after, and its relationship, if any, to earlier and later events is unknown. By far the strongest deformation in this period is proximal to the caldera complex to the north of Yucca Mountain and it is possible that the majority of this deformation, although clearly not part of a caldera per se, is nonetheless related to the activity of an early (pre-13-Ma) caldera-magmatic system rather than to regional tectonism.

13.1 to 12.7 Ma:

The interval between 13.1 and 12.7 Ma was a period of feeble tectonism in the Crater Flat area, most of which evidently is related to premonitory doming around the future (12.7-12.8 Ma) Claim Canyon caldera, source of the Paintbrush Group. The evidence for this doming is the areal variation in thickness of the voluminous tuffs emplaced in this interval because these units buried the dome as it formed (Figure 8 covers just the southern part of the dome, which is larger than the map area and is centered to the north). Immediately southward from this circumcaldera dome is a northwest-trending trough-like low across the area of dense subsurface control on northern Yucca Mountain. This low is expressed in the isopachous map of the 12.9-12.7 Ma rocks as a zone of localized thickening; however, it is also visible in the surface rocks of northern Yucca Mountain and in published mapping of this area (Scott and Bonk, 1984) as a broad, gentle fold centered on Drill Hole wash. In addition to the doming, a few minor faults have been mapped in Crater Flat that demonstrably were active between 13.1 and 12.7 Ma based on local angular unconformities and abrupt thickness changes across these faults in the volcanic section emplaced in this interval (new field data, this study).

A northwest-trending trough that is similar to the one under Yucca Mountain is expressed in the structure and isopachous maps of the Paintbrush Group on the north side of the caldera complex, under Pahute Mesa (Warren and others, 1985). The position of these two troughs, just outward from the circumcaldera dome on its north and south sides, suggests that these structures may be comparable to the rim synclines that form around salt domes. Their formation may be related to the diapiric ascent of large magma bodies into the upper crust under the area of the caldera complex.

There is suggestive evidence in several areas, especially on Yucca Mountain, that many of the major north- to northeast-striking faults of Crater Flat basin initially formed in the 13.1 to 12.7 Ma interval (C. Potter and W. Day, USGS, unpub. data). At least some of these faults appear to be growth faults within the 12.8-12.7 Ma Paintbrush Group section, based on subsurface mapping results (Fridrich, unpub. data). For most of the faults in Crater Flat basin, however, all that can be proven is that offset after deposition of the 12.7 Ma Tiva Canyon Tuff far exceeded any possible offset before 12.7 Ma.

12.7 to 11.6 Ma

A major extensional pulse occurred in the Yucca Mountain region between 12.7 and 11.6 Ma and formed the oldest structural features of the region that have present-day topographic expression. This event formed the faults that bound the northern and eastern margins of Bare

Mountain, as discussed above, as well as the majority of the closely spaced normal faults of Crater Flat basin and of Pahute Mesa, a plateau that covers most of the northern flank of the Ammonia Tanks caldera (Figures 2, 6, and 9). In addition, extreme extension occurred in the volcanic rocks on the north side of Bare Mountain in the upper plate of the Fluorspar Canyon detachment fault (the easternmost part of the Bullfrog Hills domain) during the 12.7-to-11.6 Ma event (Figure 6).

Throughout the area affected by the 12.7-11.6 Ma event, a major angular unconformity is present between the Timber Mountain Group and Paintbrush Group units. Field expressions of this unconformity include large abrupt thickness changes of the Timber Mountain units across faults, more gradual thickness changes of these units down the dip-slopes of the paleohogbacks they buried, and buttress unconformities of these units against fault scarps (Figure 10). The areal variation in the magnitude of extension that occurred in the 12.7-to-11.6 Ma event is reflected in the magnitude of angular discordance between the Paintbrush and Timber Mountain Groups, which is about 5° on Pahute Mesa. Across the northern flank of Bare Mountain (the easternmost part of the Bullfrog Hills domain), this unconformity varies from 45° to at least 70° from east to west (new field data, this study), and then diminishes to being indiscernible with the first 5 km to the west of northwest corner of Bare Mountain (D. Boden, oral comm., 1996). In Crater Flat, the angular discordance varies from as little as 10°, on northern Yucca Mountain, to values of 25-40° in the southern and northwestern parts of the basin (Figure 9).

The original pattern of extensional deformation in Crater Flat thus has a geometric pattern somewhat like a sphenochasm (a triangular pull-apart basin); it appears that the basin was pivoting open like a chinese fan with the northeast corner of the basin as the point of least extension. The complete geometry of the basin in this interval is unknown however because the Paintbrush Group is not exposed in the southwestern part of Crater Flat. If the southwest corner of the basin was also acting as a pivot point in the 12.7-to-11.6 Ma event, then the overall geometry may be like that of a rhombochasm rather than a sphenochasm.

The large-scale distributions and areal variations in the thicknesses of the major tuffs of the Timber Mountain Group (Figure 10) in Crater Flat reflect burial of a topographic form that is much like that of the modern basin. The topography tends to slope away from the caldera complex owing to circumcaldera doming and to the broad, cone-like constructional volcanic landform (the ash-flow apron) that formed around the caldera complex. Excluding those effects, the topography largely reflects the areal variation in the magnitude of extension; those areas that extended the most subsided the most.

A large volume of rock-avalanche breccia was shed off of the Bare Mountain range-front into Crater Flat in the 12.7-11.6 Ma tectonic pulse (Figure 9), as discussed above. In addition, smaller bodies of landslide and talus breccias composed of volcanic clasts are intercalated between the Paintbrush and Timber Mountain sequences and within the lowermost part of the Timber Mountain sequence in the vicinity of fault scarps within the Crater Flat basin and the easternmost part of the Bullfrog Hills domain (Figure 9; new field data, this study). These breccias are indicative of high rates of tectonism during the nearly 1-m.y.-long eruptive hiatus that separates the Paintbrush and Timber Mountain volcanic sequences.

11.6 to about 10 Ma

Extension between 11.6 and about 10 Ma in the Yucca Mountain region occurred in a belt that overlaps the belt of 12.7-to-11.6 Ma extension, but both the east and west boundaries of 11.6-to-10-Ma belt are displaced about 10 km westward of those of the preceding interval. The belt of strong extension in the 11.6-to-10-Ma interval includes only the westernmost part of Crater Flat basin, and it extends westward to the central part of the Bullfrog Hills (Figure 2).

In most of Crater Flat, the major faults active between 12.7 and 11.6 Ma continued to be active after 11.6 Ma, but at a subdued rate. This is reflected in the degree of tilting of the 11.6 Ma Rainier Mesa Tuff, which is corrected for post-10 Ma tilting in the western part of the basin (Figure 11), as well as in the much lesser fault offsets of the Rainier Mesa Tuff relative to those of the 12.7 Ma Tiva Canyon Tuff in the same areas (Scott and Bonk, 1984; Faulds and others, 1994; R. B. Scott, USGS, unpub. data; new field data, this study). Moderate to high rates of extension continued, however, in the western third of the Crater Flat basin, between the Bare Mountain range front and two major, and possibly connected faults, in the northwest and southwest parts of the basin, which were exceptionally active between 10 and 11.6 Ma (Figure 11).

To the east of those two faults, only the southeasternmost part of the basin has incurred more than about 5° of tilting since emplacement of the 11.6 Ma Rainier Mesa Tuff (Figure 11), not just between 11.6 and 10 Ma, but from 11.6 Ma to the present. Extension in the western third of the Crater Flat basin, and especially the southwesternmost area, continued at a high rate until about 10 Ma. This locally high rate of extension is reflected in large stratigraphic thickness changes of the Timber Mountain units and the 10.5 Ma basalts across the major faults in this area and by an angular unconformity between units dated at 11.45 and 10.5 Ma (new field data, this study). Rock avalanches were shed off of some major faults into the most active part of the basin during this interval (Figure 11). In the southwest part of the basin alone, it is possible that the rate of 11.6-to-10 Ma extension exceeded that of the 12.7-11.6 Ma pulse; as discussed above, no pre-11.7 Ma rocks are exposed in this area. In the rest of the basin, the majority of the total middle-Miocene-to-present extension occurred in the 12.7-to-11.6-Ma interval (Fridrich and others, 1998).

Tectonic deformation in Crater Flat basin between 11.6 and about 10 Ma did not extend as far north as the 12.7-11.6 Ma tectonism had (Figure 11). The initial trace of the Tram Ridge fault was abandoned sometime during the 12.7-11.6 Ma tectonic pulse. After 11.6 Ma, a new strand of this fault formed to the southeast and, unlike the old strand, the new one apparently did not extend all the way to the caldera complex (Figure 6). This is consistent with the much stronger activity in the southwest part of the basin between 11.6 and 10 Ma than in the northwest part of the basin. The west and south parts of the basin were areas of greater extension from the start (from 12.7-to-11.6 Ma; Figure 10); but that focus became more concentrated into the southwest part of the basin between 11.6 and 10 Ma.

The concentration of extension in the southwestern part of Crater Flat basin in the 11.6 to 10 Ma interval created an enduring physiographic distinction, in which the current area of total alluvial cover (Crater Flat physiographic feature) appears to be a distinct basin and Yucca Mountain appears to be a low range bordering that basin. In one respect, this is misleading because both the structure of the rocks and the stratigraphic record of development of that structure indicate that Yucca Mountain and Crater Flat physiographic feature have been structurally linked from the time of origin of this structural domain, between 12.7 and 11.6 Ma, to the present. It is possible, however, that the southwestern part of the basin is a structurally distinct subdomain within the Crater Flat basin - a basin within a basin - formed as a transtensional pull-apart along the southern part of the Bare mountain range front.

Basaltic volcanism began in the southwest part of Crater Flat basin during the 11.6-to-10 Ma interval, forming a thick, areally extensive sheet of layered lava flows and lesser scoria cones from which K-Ar ages of 11.3 Ma and 10.5 Ma have been obtained (Carr and Parrish, 1985; Swadley and Carr, 1987; Figure 11). These basalts are largely buried and their distribution is therefore based primarily on aeromagnetic data (V. Langenheim, USGS, written comm., 1994). The relationship of this volcanism to the tectonism is not entirely clear, but the fact that basalts are concentrated in that part of the basin that had the highest rate of extension at the time is probably significant (Fridrich and others, 1994b; 1998).

In the easternmost part of the Bullfrog Hills, the focus of extension migrated westward after 11.6 Ma, as is best shown by the westward migration of the breakaway fault for this domain, the Fluorspar Canyon fault (Figure 6). The southern part of this fault remained at the north boundary of the Bare Mountain uplift; that contact probably was not fixed in space, however, because tectonic denudation of Bare Mountain was accomplished by movement along this detachment fault, concurrent with large-magnitude extension in the upper plate. The eastern limit of the breakaway fault migrated through the upper-plate volcanic rocks, occupying at least three different positions between 12.7 and 10 Ma, each further westward with time (Figure 6). Unlike the southern part of the Fluorspar Canyon fault at the boundary of Bare Mountain, the north-to-northeast-striking breakaway strands that project off of it into the volcanic pile are largely high-angle faults and are merely the east limit of faulting and, in most cases, the approximate east limit of major tilting at the times they were active.

The fault zones that bound both the east and west sides of the Tram Ridge horst thus formed new strands with time (Figure 6). The horst originally (between 12.7 and 11.6 Ma) consisted of two separate triangular blocks at the surface, because the bounding faults on either side of the horst intersected near the surface. With time, the horst has become progressively wider owing to outward migration of the bounding faults (Figure 6).

During the westward migration of the extensional pulse across the east part of the Bullfrog Hills domain, the faulting and, especially, the apparent tilting patterns changed remarkably. Whereas the 12.7 to 11.6 Ma extension produced dominantly southeastward tilting during movement on north-northwest-dipping faults, extension from 11.6 to 11.1 Ma and from 11.1 to 10 Ma resulted in northeastward and northward tilts, respectively, during offset along faults that dip to the west-northwest.

During this westward migration of the breakaway fault system at the east limit of the Bullfrog Hills domain, the westward extent of faulting and related tilting also migrated progressively westward and reached the east flank of the Grapevine Mountains by about 8 Ma (Fridrich, unpub. data). In Miocene sections throughout the Bullfrog Hills, the major ash-flow tuff sheets are roughly conformable up to an initial unconformity and, in any one place, the oldest unconformity is the largest. But this first and largest unconformity in any one place is not the same unconformity across the whole Bullfrog Hills, but rather a series of unconformities that are progressively younger to the west (Maldonado, 1990; Maldonado and Hausback, 1990; S. Minor, USGS, unpub. data; new field data, this study). The pattern of middle to late Miocene extension in the Bullfrog Hills is thus an extension of that documented in Crater Flat basin. Extension migrated from east to west across the region and, in any one place, the trend observed during the regular westward migration is abrupt onset of a pulse of rapid extension, followed by a progressive decline in extension rate as the extensional pulse migrated away.

10 Ma to present

The magnitude of extensional fault offsets, and especially of tilting in the Crater Flat basin that has occurred from about 10 Ma to the present has been less than that of both the much shorter 11.6-to-10 Ma interval and the even shorter 12.7-to-11.6 Ma interval. Overall, therefore, the pattern has been one of progressive decline in tectonism with time after the initial extensional pulse which started shortly after 12.7 Ma, at least in the Crater Flat basin (see Fridrich and others, 1998). The structural style of activity in Crater Flat since about 10 Ma has largely been an extension of trends that began earlier (Figure 12). The number of faults showing evidence of activity is greatest for the interval from 12.7 to 11.6 Ma, intermediate from 11.6 to about 10 Ma, and least since about 10 Ma (Figure 9, 11, and 12; note that only the most active faults were shown in Figure 11). Hence, fault spacing has increased with time owing to progressive cessation of activity on minor faults. In addition, the zone of activity along the major fault systems in Crater Flat basin has retracted southward with time, especially along the Bare Mountain range front, leaving the northwest part of the basin almost completely inactive after about 10 Ma (Figures 6 and 12). The major drainages on the east side of Bare Mountain become progressively steeper (geomorphically less mature) to the south along the range front (Klinger and Anderson, 1993), suggesting that offset rates along this fault have been progressively greater as one moves southward. This interpretation is supported by Quaternary studies of sedimenatation patterns in the basin (J. Stamatakos, Southwest Research Institute, written comm., 1996). Continued movement on the southern part of the Bare Mountain fault, but not the northern part, has resulted in the relative uplift and erosional dissection of early (pre-8 Ma) basin fill in the northwest part of the Crater Flat basin (new field data, this study).

Studies documenting Quaternary rates of activity along the major fault systems in the east and central parts of Crater Flat basin (Pezzopane and others, 1994; Menges and others, 1994; A. Ramelli, NBMG, oral comm., 1995; Figure 12) show the same pattern of southward-increasing offset rates that is true for the 10 Ma-to-present interval as a whole. These studies also show that the 12.7-to-about-10-Ma pattern of left-oblique slip along these faults has continued to the present, which is geometrically required by the pivoting-open effect that is inherent in the southward increasing slip rates; the Crater Flat basin is still opening like a chinese fan. In the Quaternary and Pliocene, the southern parts of the fault systems in the eastern part of the basin have apparently been the most active structures in the basin; hence, the 3.7 and 0.1 Ma basalts apparently formed in that part of the basin that was most active at the times of these eruptions (Figure 12).

Only one structural feature has formed in the Crater Flat basin since about 10 Ma that is not obviously an extension of earlier structural patterns; namely the ridge at the southern flank of the Crater Flat physiographic feature (Figures 3 and 12). This ridge is part of the north boundary of the Amargosa Desert, which is a composite of several structural basins (Figure 2). During uplift of this ridge in southern Crater Flat, the middle to late Miocene rocks that compose the ridge have been tilted about 10° to the north; this is the major tilting that has occurred in the Crater Flat basin since about 10 Ma (Figure 12). The southern scarp of this ridge is continuous with the scarp along the southwestern boundary of the Bare Mountain uplift, which is the northeastern boundary of the western Amargosa basin (Figure 12). These scarps have been interpreted as being related to a structure called the Highway 95 fault, as discussed above. If this structure is real, it is concealed under Quaternary alluvium and has no discernible surface trace through these young sediments.

Evidence of recent offset on all of the Quaternary faults in the basin ends across this ridge at the southern margin of Crater Flat physiographic feature. Hence, the south-central part of the Crater Flat basin has been an isolated pocket of faulting activity in the late Quaternary. Moreover, the late Quaternary rate of tectonic activity in Crater Flat basin is feeble. Based on fault-slip studies, the late Quaternary rate of northwest-southeast lengthening (horizontal offset) across the southern part of the basin, where the rate is at a maximum, is approximately 0.1 meter per thousand years (Menges and others, 1994; Fridrich and others, 1998). The late Quaternary extension rate is approximately half as great across central Yucca Mountain, and an order of magnitude lower across northern Yucca Mountain (Fridrich and others, 1998).

Many of the proximal physiographic features of the Yucca Mountain area took on their basic topographic form between 12.7 and 10 Ma; this includes Yucca Mountain itself, Crater Flat physiographic feature, and Bare Mountain. However, a substantial part of the topography of the greater Yucca Mountain region was created in the interval from about 10 Ma to present, especially the first half of this interval. For example, proceeding clockwise, Death Valley, Sarcobatus and Gold Flats, Kawich and Emigrant Valleys, and French Flat (Figure 2) are post-10 Ma basins at least in the sense that they evidently assumed their modern topographic form near the end of the Miocene.

These younger basins mark a clear departure in structural style from the 12.7-to-10 Ma tectonism that was concentrated in the area of the southwest Nevada volcanic field; specifically, the tilted-domino style of deformation along closely spaced faults was apparently replaced by classic large-scale Basin-Range block faulting in areas to the north and east of Yucca Mountain, and formation of large strike-slip pull-apart basins, to the west and south. Possible underlying causes for this change are: (1) The volcanic field has been in a waning cycle since 11 Ma and especially since 7.5 Ma, the age of the last major silicic volcanism; hence, the mechanical behavior of the crust has been changing as it cooled, and (2) after 10 Ma the tectonic pulse migrated out of the area of the volcanic field into areas of the crust that were structurally and mechanically different throughout the Cenozoic.

SUMMARY AND DISCUSSION OF TECTONIC MODELS

During the late Cenozoic, the Yucca Mountain region has evolved as a mosaic of structural domains. These domains are separated by bounding structures or zones across which abrupt changes are present in the timing, magnitude, and style of extension and other deformation. Some of these domain boundaries, such as the Bare Mountain range-front fault, have remained active over long periods of time, and have maintained much of their original character despite changes in the patterns of tectonism in the surrounding region. Others, such as the breakaway fault of the

Bullfrog Hills domain, have changed in their geometry over time, and still others have come and gone as the dynamics of deformation in the region has changed.

The focus of maximum extension migrated westward through the Yucca Mountain region over a major part of the late Cenozoic. For at least the period of about 13 to about 10 Ma and for the area of the southwest Nevada volcanic field, this migration took the form of a steadily advancing front that moved across the region like a wave, migrating both within individual structural domains, and across domain boundaries. At other times, such as from about 10 Ma to present, it is only the focus of maximum extension rate that appeared to show any regular pattern of migration, and activity behind the advancing front, now located in the Death Valley area, has been scattered and irregular.

In any place, the evident trend during the westward migration is abrupt onset of a pulse of rapid extension, followed by a progressive but slower decline in extension rate as the extensional pulse migrated away. Scattered small domains, including a major part of Crater Flat basin, have remained tectonically active at feeble rates long after passage of an extensional pulse.

The structural style of extension in the Crater Flat basin has progressively changed during its tectonic evolution; specifically, fault spacing has increased with time and the rate of tilting has decreased. Moreover, the area of active tectonism in the basin has been progressively shrinking; whereas the 12.7-to-11.6 Ma peak phase of tectonism involved strong deformation throughout Crater Flat basin, extension since 11.6 Ma has only involved approximately half of the original area of the basin, and the majority of the deformation has been concentrated in less than half of that area. Stratigraphic units younger than 10 Ma are little exposed and difficult to date; hence, there are large uncertainties in the constraints on the waning phase of evolution of the basin, especially for the interval between 10 and 4 Ma.

An oddity of the Crater Flat basin is that more than two-thirds of the thick Tertiary "basin fill" in Crater Flat was deposited before the formation of this structural basin. Most of the volcanic section, and all of the prevolcanic sedimentary section under Crater Flat and Yucca Mountain date back to a period before the 12.7-to-11.6-Ma event in which Bare Mountain was uplifted and tectonically denuded, and Crater Flat basin subsided. Existing data appears consistent with the hypothesis of Hamilton (1989) that the pre-12.6 Ma volcanic rocks of the Bullfrog Hills domain slid off of Bare Mountain to the west and north along the Fluorspar Canyon detachment fault, and hence were contiguous with the volcanic rocks to the east of Bare Mountain, in Crater Flat, before the 12.7-11.6 Ma extensional pulse. The greater thickness of this pre-12.6 Ma Tertiary section in western Crater Flat basin and the Bullfrog Hills, relative to surrounding areas, suggests this area was a depositional basin of some kind, but additional work would be required to reconstruct what the area looked like before the 12.7-11.6 Ma tectonic event, and to determine whether Hamilton's hypothesis is in fact accurate.

None of the concealed master structures that have been invoked by previous workers to explain the structural characteristics of Crater Flat basin can be proven or disproven based on available data. However, it is possible to address two important questions: (1) Is it necessary to invoke concealed structures to explain the observed features of the Crater Flat basin?, and (2) Is the question of whether these concealed features are present or not important to understanding the Crater Flat basin, particularly for the evaluation of seismic hazards for the Yucca Mountain site?

With respect to the caldera hypothesis, any caldera that is concealed under Crater Flat must be related to the 13.1 to 13.5 Ma Crater Flat Group or to older, underlying units because the caldera sources of all major younger units have been identified (Sawyer and others, 1994). The inferred concealed caldera therefore would not only have predated the formation of the Crater Flat basin, but it would have been a fossil structure when this basin formed. Hence, the question of whether a caldera is concealed under Crater Flat is irrelevant both to understanding the Crater Flat basin and to evaluating seismic hazards for the Yucca Mountain site.

With respect to the detachment hypothesis, the creation of Crater Flat basin and the uplift of Bare Mountain all occurred within the 1 m.y. period from 12.7 to 11.6 Ma. Hence, if the inferred detachment fault under the Crater Flat basin was once rooted to the west, the uplift of Bare Mountain severed the detachment almost immediately after the basin formed. Once it was truncated by the range-front fault, the hypothetical detachment fault under Crater Flat basin would have been a rootless structure, and there would have been no kinematic reason for significant additional movement to occur along it.

Recent mapping (new field data, this study) that was done in part to test the detachment hypotheses of Hamilton (1989) and Scott (1990) has documented a number of field relations that are difficult to reconcile with these hypotheses: (1) The detachment fault system of the Bullfrog Hills appears to have had an eastern termination in the vicinity of the Bare Mountain range-front fault, as discussed above, rather than continuing to the east under Crater Flat and Yucca Mountain. (2) The postulated detachment fault under Crater Flat and Yucca Mountain was interpreted as being located at the basal Tertiary contact. However, gravity and bore-hole data indicate this contact was offset by high-angle faults in the 14 to 13.1 Ma tectonic event, before the creation of Crater Flat basin, which probably would have prevented it from becoming a detachment fault.

Moreover, the proposed detachment fault under Yucca Mountain and Crater Flat was not interpreted from any direct evidence. Rather, it was invoked based on the supposition that, because the Crater Flat domain has a tilted-domino structural style that resembles that of many areas of extreme extension and detachment faulting, it must therefore have a detachment fault under it. This structural style is, however, found throughout the southwest Nevada volcanic field wherever the extensional faults formed during or shortly after the peak in eruptive activity. In the Crater Flat basin, as in much of the volcanic field, this structural style is developed at low percentages of extension, in some cases less than 10%. Detachment faulting at such low percentages of extension appears unlikely.

Rather than being an indicator of detachment faulting, the development of a tilted-domino structural style along closely spaced faults during regional extension may reflect the influence of large-scale crustal magmatism. Specifically, magmatism may alter the style of crustal deformation by changing the thermal gradient, pore pressures, and other conditions that influence the strength of the crust and the state of stress in it. The common presence of the tilted-domino structural style in many areas of extreme extension may indicate that crustal magmatism played a role in the creating the conditions for detachment faulting in these areas, as suggested by Parsons and Thompson (1993).

A common implication of both the caldera and detachment fault hypotheses is that the observed surface structures of the Crater Flat area terminate in the subsurface against a master structure in the upper crust. The only ground-truth evidence that can be applied to test this implication was supplied by the 1992 earthquake at Little Skull Mountain, about 10 km east of Yucca Mountain. The focus of this earthquake was located at 12 km depth, and aftershocks defined a planar fault surface with a dip of about 65° extending from 12 km into the upper crust

(Harmsen, 1994). These data are compelling evidence that the high-level faults of the Yucca Mountain region do not terminate against any upper-crustal structure; rather, they extend down to the middle crust, as they do is the rest of the southern Great Basin (Harmsen and Bufe, 1992).

A question could be posed as to whether the deep (10-15 km) seismogenic basement in the Yucca Mountain region is a detachment fault or merely the brittle-ductile transition. This question is unanswerable and, moreover, is irrelevant both to understanding the origin of Crater Flat basin and to evaluating seismic hazards for the Yucca Mountain site.

The strong southwestward increase in vertical-axis rotation within Crater Flat basin, coupled with the evident abrupt termination of this distributed strike-slip deformation at the west and south boundaries of the basin, is strong suggestive evidence of the presence of a major strike-slip fault at either or both of these two boundaries. If so, however, the strike-slip structure(s) is totally concealed. The presence of such a structure would be relevant both to the origin of Crater Flat basin and to the evaluation of seismic hazards for the Yucca Mountain site. Testing alternative hypotheses that a concealed major strike-slip fault is associated with the Crater Flat basin would, however, require additional study. The pattern of oroflexural bending in this basin does not require that a master strike-slip fault be present; the strike-slip deformation in the Crater Flat basin may simply be distributed rather than discrete.

CONCLUSION

Whereas virtually all of the previously proposed theories for the tectonics of the Crater Flat area have tried to explain the structural features of this area in terms of end-member models, the field-geologic and geophysical evidence indicates that Crater Flat basin is not an end-member example of anything; it is a hybrid basin of complex origin. Structurally, the Crater Flat basin reflects three major influences: (1) east-west- to northwest-southwest-directed extension, (2) northwest-directed dextral deformation, and (3) doming around the caldera complex, which also acted a pivot point for oblique extension. This mixture of influences is consistent with the setting of this basin on the flank of a large caldera complex that was active during its formation, and within the Walker Lane belt near the boundary between this province, which is characterized by both strike-slip deformation and extension, and the northern Basin-and-Range province, which is characterized by more purely extensile deformation. The range-front-like fault at the western boundary of Crater Flat basin appears to form the eastern limit of extreme extension, detachment faulting, and large-scale isostatic uplift, as discussed above. Thus, although the Crater Flat basin probably is not underlain by a detachment fault, detachment faulting may nonetheless have played an important role in the formation of this basin.

Whereas it is impossible to disprove the presence of a concealed caldera or a detachment fault under Crater Flat, there is in fact nothing in the existing data that requires their invocation. There also is no clearcut evidence for a master strike-slip fault through this basin or at its boundaries; however, distributed strike-slip deformation has played a major role in creating the Crater Flat basin, and it continues to play a role in the tectonics of this basin. Determining the significance of the strike-slip deformation in this basin, with respect to the basin's origin and to seismic risk assessment for the Yucca Mountain site, will require approaching the problem with a more regional view than was done in this study.

ACKNOWLEDGMENTS

I thank colleagues in the USGS, especially Dennis O'Leary, for numerous critical discussions of the tectonics of the Yucca Mountain region. Helpful reviews of the manuscript were provided by Lauren Wright, Christopher Potter, Thomas Hoisch, Mark Hudson, Ed DeWitt, and Bruce Crowe. Jason Price, Michele Murray, F. William Simonds, and Chris Hildenbrand assisted the author in the field. Funding was provided by the U. S. Department of Energy Yucca Mountain Project.

REFERENCES CITED

Ackerman, H. D., Mooney, W. D., Snyder, D. B., and Sutton, V. D., 1988, Preliminary interpretation of seismic-refraction and gravity studies west of Yucca Mountain, Nevada and California, *in*, Carr, M. D., and Yount, J. C., eds., Geologic and Hydrologic Investigations of a potential Nuclear Waste Disposal Site at Yucca Mountain, Nevada: U. S. Geological Survey Bulletin 1790, p. 23-33.

Blakely, R. J., Jachens, R. C., Calzia, J. P., and Langenheim, V. E., in press, Cenozoic basins of the Death Valley extended terrane as reflected in regional-scale gravity anomalies: Geological Society of America Special Paper: Cenozoic Basins of the Death Valley Region.

Broxton, D. E., Warren, R. G., Byers, F. M., Jr., and Scott, R. B., 1989, Chemical and mineralogic trends within the Timber Mountain-Oasis Valley caldera complex, Nevada: Evidence for multiple cycles of chemical evolution in a long-lived silicic magma system: Journal of Geophysical Research, v. 94, no. B5, p. 5961-5986.

Burchfiel, B. C., Hamill, G. S., IV, and Wilhelms, D. E., 1983 Structural geology of the Montgomery Mountains and the northern half of the Nopah and Resting Spring Ranges, nevada and California: Geological Society of America Bulletin, v. 94, p. 1359-1376.

Carr, M. D., Waddell, S. J., Vick, G. S., Stock, J. M., Monsen, S. A., Harris, A. G., Cork, B. W. and Byers, F. M., Jr., 1986. Geology of drill hole UE25-p#1, a test hole in pre-Tertiary rocks near Yucca Mountain, southern Nevada: U.S. Geological Survey Open-File Report 86-175, 102 p.

Carr, W. J., 1982, Volcano-tectonic history of Crater Flat, southwestern Nevada, as suggested from new evidence from drill hole USW VH-1 and vicinity: U. S. Geological Survey Open-File Report 82-457, 23 p.

Carr, W. J., 1990, Styles of extension in the Nevada Test Site region, southern Walker Lane belt; An integration of volcano-tectonic and detachment fault models, *in*, Wernicke, B. P., ed., Basin and range extensional tectonics near the latitude of Las Vegas, Nevada: Geological Society of America Memoir 176, p. 283-303.

Carr, W. J. and Parrish, L. D., 1985, Geology of drill hole USW VH-2, and structure of Crater Flat, southwestern Nevada:U. S. Geological Survey Open-File Report 85-475, 41 p.

Carr, W. J., Byers, F. M. Jr., and Orkild, P. P., 1986, Stratigraphic and volcano-tectonic relations of Crater Flat Tuff and some older volcanic units, Nye County, Nevada: U. S. Geological Survey Professional paper 525B, p. B43-B48.

Chapin, C. E. and Lowell, G. R., 1979, Primary and secondary flow structures in ash-flow tuffs of the Gribbles Run paleovalley, central Colorado: *in,* Smith, R. L., ed., Ash-flow Tuffs, Geological Society of America Special Paper 180, p. 137-154.

Christiansen, R. L., and Lipman, P. W., 1965, Geologic map of the Topopah Spring, NW quadrangle, Nye County, Nevada: U. S. Geological Survey Map GQ-444: scale 1:24,000.

Christiansen, R. L., Lipman, P. W., Orkild, P. P., and Byers, F. M., Jr., 1965, Structure of the Timber Mountain caldera, southern Nevada and its relation to Basin-Range structure: U. S. Geological Survey Professional Paper 525-B, p. B43-48.

Cornwall, H. R., 1972, Geology and mineral deposits of southern Nye County, Nevada: Nevada Bureau of Mines and Geology Bulletin 77, 49 p., 1 plate.

Craig, R. W., Reed, R. L. and Spengler, R. W., 1983. Geohydrologic data for test well USW H-6, Yucca Mountain area, Nye County, Nevada: U.S. Geological Survey Open-File Report 83-856, 39 p.

Crowe, B. M., Perry, F. V., Geissman, J., McFadden, L. D., Wells, S. G., Murrell, M., Poths, J., Valentine, G. A., Bowker, L., and Finnegan, K., 1995, Status of volcamism studies for the Yucca Mountain site characterization project: Los Alamos National Laboratories report LA-12908-MS, Los Alamos, New Mexico, 363 p.

Cummings, D., 1968, Mechanical analysis of the effect of the Timber Mountain caldera on Basin and Range faults: Journal of Geophysical Research, v. 73, p. 2787-2794.

Day, W. C., Potter, C. J., Sweetkind, D. S., Dickerson, R. P., San Juan, C. A., and Scott, R. B., in press, Bedrock geologic map of the central block area, Yucca Mountain, Nevada: U. S. Geological Survey, Miscellaneous Investigations Map I - 2601, 2 plates with text, Scale 1:6000.

Ekren, E. B., Orkild, P. P., Sargent, K. A., and Dixon, G. L., 1977, Geologic map of the Tertiary rocks, Lincoln County, Nevada: U. S. Geological Survey Miscellaneous Investigations Series Map I-1041, scale 1:250,000.

Faulds, J. E., Bell, J. W., Feuerbach, D. L., and Ramelli, A. R., 1994, Geologic map of the Crater Flat area, Nye County, Nevada: Nevada Bureau of Mines and Geology Map 101, 1:24,000 scale.

Fridrich, C. J., Dudley, W. W., Jr., and Stuckless, J. S., 1994a, Hydrogeologic analysis of the saturated-zone ground-water system, under Yucca Mountain, Nevada: Journal of Hydrology, v. 154, p. 133-168.

Fridrich, C. J., Crowe, B. M., Hudson, M. R., Langenheim, V. E., and Thompson, G. A., 1994b, Structural control of basaltic volcanism in a region of oblique extension, southwest Nevada volcanic field: [abstr] EOS, Transactions of the American Geophysical Union, v. 75, p. 603.

Fridrich, C. J., Whitney, J. W., Hudson, M. R., and Crowe, B. M., 1998, Space-time patterns of Late Cenozoic extension, vertical-axis rotation, and volcanism in the Crater Flat basin, southwest Nevada: U. S. Geological Survey Open-File Report 98-xxx.

Fridrich, C. J., Grauch, V. J. S., and Sawyer, D. A., 1996, Geophysical domains of the Nevada Test Site region and applications to regional hydrology: [abstr] Geological Society of America Abstracts with Programs, v. 28, no. 7, p. 92.

Frizzell, V. A., Jr., and Schulters, J., 1990, Geologic map of the Nevada Test Site, southern Nevada: U. S. Geological Survey Map I-2046, 1:100,000 scale.

Grauch, V. J. S., Sawyer, D. A., Hudson, M. R., Minor, S. A., and Cole, J. C., 1993, New detailed aeromagnetic data give fresh insight to mapping covered geologic units in the southwestern Nevada volcanic field: [abstr] American Geophysical Union (EOS), v. 74, p. 221.

Hamilton, W. B., 1988, Detachment faulting in the Death Valley region, California and Nevada: *in*, Carr, M. D., and Yount, J. C., eds, Geologic and hydrologic investigations of a potential nuclear waste disposal site at Yucca Mountain, southern Nevada: U. S. Geological Survey Bulletin 1790, p. 51-86.

Harmsen, S. C., 1994, The Little Skull Mountain earthquake of 29 June 1992: Aftershock focal mechanisms and tectonic stress field implications: Bulletin of the Seismological Society of

America, v. 84, no. 5, p. 1484-1505.
Harmsen, S. C., and Bufe, C. G., 1992, Seismicity and focal mechanisms in the southern Great Basin of Nevada and California: 1987 through 1989: U. S. Geological Survey Open-File Report 91-572, 216 p.
Hinrichs, E. N., 1968, Geologic map of the Camp Desert Rock quadrangle, Nye County, Nevada: U. S. Geological Survey Map GQ-726, 1:24,000 scale.
Hoisch, T. D., Heizler, M. T., and Zartman, R. E., 1997, Timing of detachment faulting in the Bullfrog Hills and Bare Mountain area, southwest Nevada: Inferences from $^{40}Ar/^{39}Ar$, K-Ar, and fission-track thermochronology: Journal of Geophysical Research, v. 102, p. 2815-2833.
Hudson, M. R., Sawyer, D. A., and Warren, R. G., 1994, Paleomagnetism and rotation constraints for the middle Miocene southwestern Nevada volcanic field: Tectonics, v. 13, p. 258-277.
Jenkins, O. P., 1962, Geologic map of California, Trona Sheet: California Division of Mines and Geology, scale 1:250,000.
Klinger, R. E. and Anderson, L. W., 1993, Preliminary evaluation of the Bare Mountain fault zone, Nye County, Nevada: Seismotectonic Report 93-6, Bureau of Reclamation, Denver, Colorado, 15 p.
Lipman, P. W., 1984, The roots of ash-flow calderas in western North America: Windows into the tops of granitic batholiths: Journal of Geophysical Research, v. 89, p. 8801-8841.
Lobmeyer, D. H., Whitfield, M. S., Jr., Lahoud, R. G., and Bruckheimer, L., 1983, Geohydrologic data for test well UE-25b-1, Nevada Test Site, Nye County, Nevada: U. S. Geological Survey Open-File Report 83-855, 52 p.
Longwell, C. R., Pampeyan, E. H., Bowyer, B., and Roberts, R. J., 1965, Geology and mineral deposits of Clark County, Nevada: Nevada Bureau of Mines and Geology Bulletin 62, 218 p., 16 plates.
Maldonado, F., 1990, Geologic map of the northwest quarter of the Bullfrog 15-minute quadrangle, Nye County, Nevada: U. S. Geological Survey Miscellaneous Investigations Series Map I-1985, scale 1:24,000.
Maldonado, F. and Hausback, B. P., 1990, Geologic map of the northeast quarter of the Bullfrog 15-minute quadrangle, Nye County, Nevada: U. S. Geological Survey Miscellaneous Investigations Series Map I-2049, scale 1:24,000.
Maldonado, F., and Koether, S. L., 1983, Stratigraphy, structure, and some petrologic features of Tertiary volcanic rocks at the USW G-2 drill hole, Yucca Mountain, Nevada: U. S. Geological Survey Open-File Report 83-732, 93 p.
Menges, C. M., Wesling, J. R., Whitney, J. A., Swan, F. H., Coe, J. A., Thomas, A. P., and Oswald, J. A., 1994, Preliminary results of paleoseismic investigations of Quaternary faults on eastern Yucca Mountain, Nye County, Nevada: High-Level Radioactive Waste Management, Proceedings of the Fifth Annual International Conference, American Nuclear Society, Las Vegas, Nevada, v. 4, p. 2373-2390.
Minor, S. A., Sawyer, D. A., Wahl, R. R., Frizzell, V. A., Jr., Schilling, S. P., Warren, R. G., Orkild, P. P., Coe, J. A., Hudson, M. R., Fleck, R. J., Lanphere, M. A., Swadley, W C, and Cole, J. C., 1993, Preliminary geologic map of the Pahute Mesa 30' x 60' Quadrangle, Nevada: U. S. Geological Survey Open-File Report 93-299.

Monsen, S. A., Carr, M. D., Reheis, M. C., and Orkild, P. P., 1992, Geologic map of Bare Mountain, Nye County, Nevada: U. S. Geological Survey Miscellaneous Investigations Series Map I-2201, scale 1:24,000.

Parsons, T., and Thompson, G. A., 1993, Does magmatism influence low-angle normal faulting?: Geology, v. 21, p. 247-250.

Pezzopane, S. K., Menges, C. M., and Whitney, J. W., 1994, Quaternary paleoseismology and Neogene tectonics at Yucca Mountain, Nevada: Proceedings of the Workshop on Paleoseismology, September 18-22, 1994, Marshall, California, National Earthquake Hazards Reduction Program, U. S. Geological Survey Open-File Report 94-568, p. 149-151.

Piety, L. A., 1993, Compilation of known and suspected Quaternary faults within 100 km of Yucca Mountain: U. S. Geological Survey Open-File Report 94-112, 404 p., 2 plates.

Reynolds, M. W., 1969, Stratigraphy and structural geology of the Titus and Titanothere Canyons area, Death Valley, California [Ph.D. dissert.]: Berkeley, University of California, Berkeley, CA, 310 p.

Rosenbaum, J. G., Hudson, M. R., and Scott, R. B., 1991, Paleomagnetic constraints on the geometry and timing of deformation at Yucca Mountain, Nevada: Journal of Geophysical Research, v. 96, p. 1963-1980.

Rush, F. E., Thordarson, W., and Pyles, D. G., 1984. Geohydrology of test well USW H-1, Yucca Mountain, Nye County, Nevada: U.S. Geological Survey Water-Resources Investigations Reports 84-4032, 62 p.

Sawyer, D. A., Fleck, R. J., Lanphere, M. A., Warren, R. G., Broxton, D. E., and Hudson, M. R., 1994, Episodic caldera volcanism in the Miocene southwest nevada volcanic field: Revised stratigraphic framework, $^{40}Ar/^{39}Ar$ geochronologic framework, and implications for magmatism and extension: Geological Society of America Bulletin, v. 106, no. 10, p. 1304-1318.

Schweickert, R. A. 1989, Evidence for a concealed strike-slip fault beneath Crater Flat, Nevada: Geological Society of America Abstracts with Programs, v. 21, no. 9., p. A90.

Scott, R. B., 1990, Tectonic setting of Yucca Mountain, southwest Nevada, *in*, Wernicke, B. P., ed., Basin and range extensional tectonics near the latitude of Las Vegas, Nevada: Geological Society of America Memoir 176, p. 251-282.

Scott, R. B., and Bonk, J., 1984, Preliminary geologic map of Yucca Mountain with geologic sections, Nye County, Nevada: U. S. Geological Survey Open-File Report 84-494, 1:12,000 scale.

Scott, R. B. and Castellanos, M., 1984, Stratigraphic and structural relations of volcanic rocks in drill holes USW GU-3 and USW G-3, Yucca Mountain, Nye County, Nevada: U.S. Geological Survey Open-File Report 84-491, 136 p.

Simonds, F. W., Whitney, J. W., Fox, K. F., Ramelli, A. R., Yount, J. C., Carr, M. D., Menges, C. M., Dickerson, R. P., and Scott, R. B., 1995, Map showing fault activity in the Yucca Mountain area, Nye County, Nevada: U. S. Geological Survey map I-2520, scale 1:24,000.

Smith, R. L., and Bailey, R. A., 1968, Resurgent cauldrons: Geological Society of America Memoir 116, p. 613-662.

Snyder, D. B., and Carr, W. J., 1984, Interpretation of gravity in a complex volcano-tectonic setting, southwestern Nevada: Journal of Geophysical Research, v. 89, no. B12, p. 10193-10206.

Spengler, R. W., Byers, F. M., Jr. and Warner, J. B., 1981. Stratigraphy and structure of volcanic rocks in drill hole USW-G1, Yucca Mountain, Nevada: U.S. Geological Survey Open-File Report 81-1349, 50 p.

Stewart, J. H., 1988, Tectonics of the Walker Lane belt, western Great Basin-Mesozoic and Tertiary deformation in a zone of shear, *in*, Ernst, W. G., ed., Metamorphism and crustal evolution of the western United States, Rubey Vol. VII: Englewood Cliffs, New Jersey, Prentice Hall, p. 683-713.

Streitz, R. and Stinson, M. C., 1974, Geologic map of California, Death Valley sheet: California Division of Mines and Geology, scale 1:250,000.

Swadley, W C, and Carr, W. J., 1987, Geologic map of the Quaternary and Tertiary deposits of the Big Dune Quadrangle, Nye County, Nevada and Inyo County, California: U. S. Geological Survey Map I-1767: scale 1:48,000.

Thordarson, William, Rush, F.E., Spengler, R.W. and Waddell, S.J., 1984. Geohydrologic and drill hole data for test well USW H-3, Yucca Mountain, Nye County, Nevada: U.S. Geological Survey Open-File Report 84-149, 28 p.

Warren, R. G., Byers, F. M., Jr., and Orkild, P. P., 1985, Post-Silent Canyon caldera structural setting for Pahute Mesa: *in,* Third Symposium on Containment of Underground Nuclear Explosions, Idaho Operations Office of the DOE, Idaho Falls, Idaho, v. 2, p. 3-30.

Weiss, S. I., Noble, D. C., Worthington, J. E., IV, and McKee, E. H., 1993, Neogene tectonism from the southwestern Nevada volcanic field to the White Mountains, California, Part 1. Miocene volcanic stratigraphy, paleotopography, extensional faulting, and uplift between northern Death Valley and Pahute Mesa: *in*, Lahren, M. M., Trexler, J. H., Jr., and Spinosa, C., eds., Crustal Evolution of the Great basin and Sierra Nevada: Cordilleran/Rocky Mountain Section, Geological Society of America Guidebook, Department of Geological Sciences, University of Nevada, Reno, p 353-382.

Winograd, I. J., and Thordarson, W., 1975, Hydrogeologic and hydrochemical framework, south-central Great Basin, Nevada-California, with special reference to the Nevada Test Site: U. S. Geological Survey Professional Paper 712-C, 125 p.

Wright, L. A., 1989, Overview of the role of strike-slip and normal faulting in the Neogene history of the region northeast of Death Valley, California-Nevada, *in,* Ellis, M. A., ed., Late Tertiary evolution of the southern Great Basin, Nevada Bureau of Mines and Geology Open File 89-1, p. 1-11.

Wright, L. A. and Troxel, B. W., 1993, Geologic map of the Funeral Mountains and adjacent areas, Death Valley region, southern California: U. S. Geological Survey Miscellaneous Investigations Series map I-2305, scale 1:24,000.

FIGURE CAPTIONS

Figure 1: Location of Yucca Mountain (star) in the southwest Nevada volcanic field (Broxton and others, 1989) of the western Great Basin, with schematic representations of faults of the Walker Lane Belt that have strike-slip components of offset (dip-slip offsets not shown), modified from Stewart (1988).

Figure 2: Generalized map of the Yucca Mountain region showing major physiographic features and faults; compiled from Jenkins, 1962; Longwell and others, 1965; Cornwall, 1972; Streitz and Stinson, 1974; Ekren and others, 1977; Burchfiel and others, 1983; Wright, 1989; Frizzell and Schulters, 1990; Piety, 1993; Sawyer and others, 1994.

Figure 3: Map showing structural domains and domain boundaries of the Yucca Mountain region and internal fault structures of the Crater Flat basin and selected parts of adjacent domains; compiled from Monsen and others, 1992; Simonds and others, 1995; and Fridrich and others, unpub. data.

Figure 4: Schematic illustrations of (A) resolved sense of strike-slip shear on faults having a range of orientations, given a representational stress ellipsoid for the western Great Basin, and (B) illustration showing the dynamic sense of strike-slip shear along originally north-striking faults when the same stress regime results in vertical axis rotation concurrent with extension.

Figure 5: Structure map of Bare Mountain; modified from Monsen and others, 1992; Fridrich and others, unpub. data. Data on metamorphic grades modified from Hoisch (this volume).

Figure 6: Structure map of Tram Ridge horst and neighboring areas, showing the migration of activity on the Bare Mountain-Tram Ridge fault system and the Fluorspar Canyon fault system. Compiled from Monsen and others, 1992; Fridrich and others, unpub. data.

Figure 7: Map showing features relevant to tectonic activity from 13 to 14+ Ma, including thicknesses from the top of the Lithic Ridge Tuff to the top of the Tram Tuff in bore holes under Yucca Mountain, outcrop areas of volcanic rocks older than 13 Ma in the Crater Flat basin and vicinity, and faults active from 13.1 to 14+ Ma. Compiled from Fridrich and others, 1994a; unpub. data.

Figure 8: Map showing features relevant to tectonic activity from 12.7 to 13.1 Ma, including contoured thickness from the top of the 13.1 to 13.5 Ma Crater Flat Group to the top of the 12.7 to 12.8 Ma Paintbrush Group in the Crater Flat basin, and a very local angular unconformity formed in this time interval, as well as faults that were active between 12.7 and 13.1 Ma. Map data compiled from Carr, 1982; Carr and

Parrish, 1985, Fridrich and others, unpub. data; and Scott and Bonk, 1984. Subsurface data compiled from Spengler and others, 1981; Craig and others, 1983; Lobmeyer and others, 1983; Maldonado and Koether, 1983; Rush and others, 1984; Scott and others, 1984; Thordarson and others, 1984; M. Carr and others, 1986.

Figure 9: Map showing features relevant to tectonic activity from 12.7 to 11.6 Ma in Crater Flat basin and vicinity. Faults in Claim Canyon caldera are predominantly related to caldera resurgence which occurred between 12.7 and 12.5 Ma. Dips in the Claim Canyon caldera reflect resurgent doming of the cauldron block. Faults shown in Crater Flat basin are ones known to have been active in this interval based on angular unconformities between the 12.7 Ma Tiva Canyon Tuff and the 11.4-11.7 Ma Timber Mountain Group. Attitudes in Crater Flat are those of the Tiva Canyon Tuff corrected for tilting after 11.6 Ma; with that correction, these attitudes represent the degree of angular unconformity between the Paintbrush and Timber Mountain Groups in Crater Flat. Also shown are the locations and suspected sources areas of rock-avalanche breccias formed in this time interval. Map data compiled from Christiansen, and Lipman, 1965; Scott and Bonk, 1984; Fridrich and others, unpub. data; Scott, R. B., unpub. data).

Figure 10: Map showing distributions of the 11.6 Ma Rainier Mesa Tuff, with thicknesses in meters, as well as the distribution of the 11.45 Ma Ammonia Tanks Tuff in Crater Flat basin. The distributions and thickness variations in these units reflect primarily the topography that these units buried, and that was created by faulting, tilting, uplift, and subsidence from 12.7 to 11.6 Ma. Compiled from Scott and Bonk, 1984; Faulds and others, 1994; Fridrich and others, unpub. data; R. B. Scott, USGS, unpub. data).

Figure 11: Map showing features relevant to tectonic activity from 11.6 to about 10 Ma in Crater Flat basin, including attitudes of the 11.6 Ma Rainier Mesa Tuff, corrected for post-10 Ma tilting, and distibution of 11.3-to-10.5 Ma basalts. Most of the faults active from 12.7-11.6 Ma (Figure 10) were active to some degree from ~10-11.6 Ma as well; this figure shows only those faults that were active enough from about-10-to-11.6 Ma that there are very large thickness changes or changes in tilting across them, or their activity resulted in rock-avalanching in this time interval. Compiled from Scott and Bonk, 1984; Faulds and others, 1994; Fridrich and others, unpub. data; R. B. Scott, USGS, unpub. data).

Figure 12: Map showing features relevant to tectonic activity from about 10 Ma to present in Crater Flat basin, including tilting, active faults, and basalts erupted. Compiled from Faulds and others, 1994; F. W. Simonds and R. B. Scott, USGS, written comm., 1995; Fridrich and others, unpub. data; R. B. Scott, USGS, unpub. data; Menges and others, 1994).

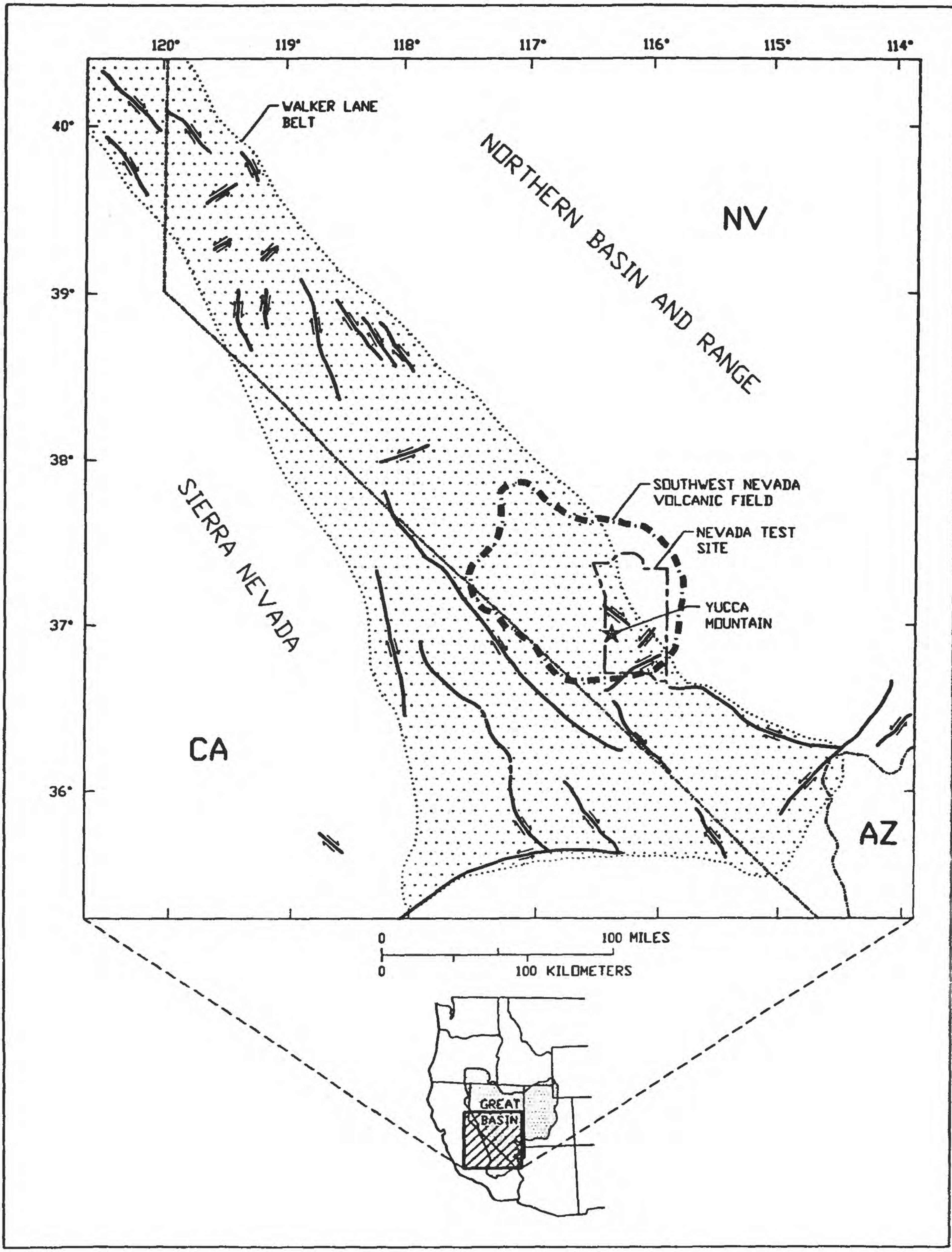
120°
119°
118°
117°
116°
115°
114°
40°
39°
38°
37°
36°
WALKER LANE BELT
NORTHERN BASIN AND RANGE
NV
SIERRA NEVADA
SOUTHWEST NEVADA VOLCANIC FIELD
NEVADA TEST SITE
YUCCA MOUNTAIN
CA
AZ
0
100 MILES
0
100 KILOMETERS
GREAT BASIN

Figure 1

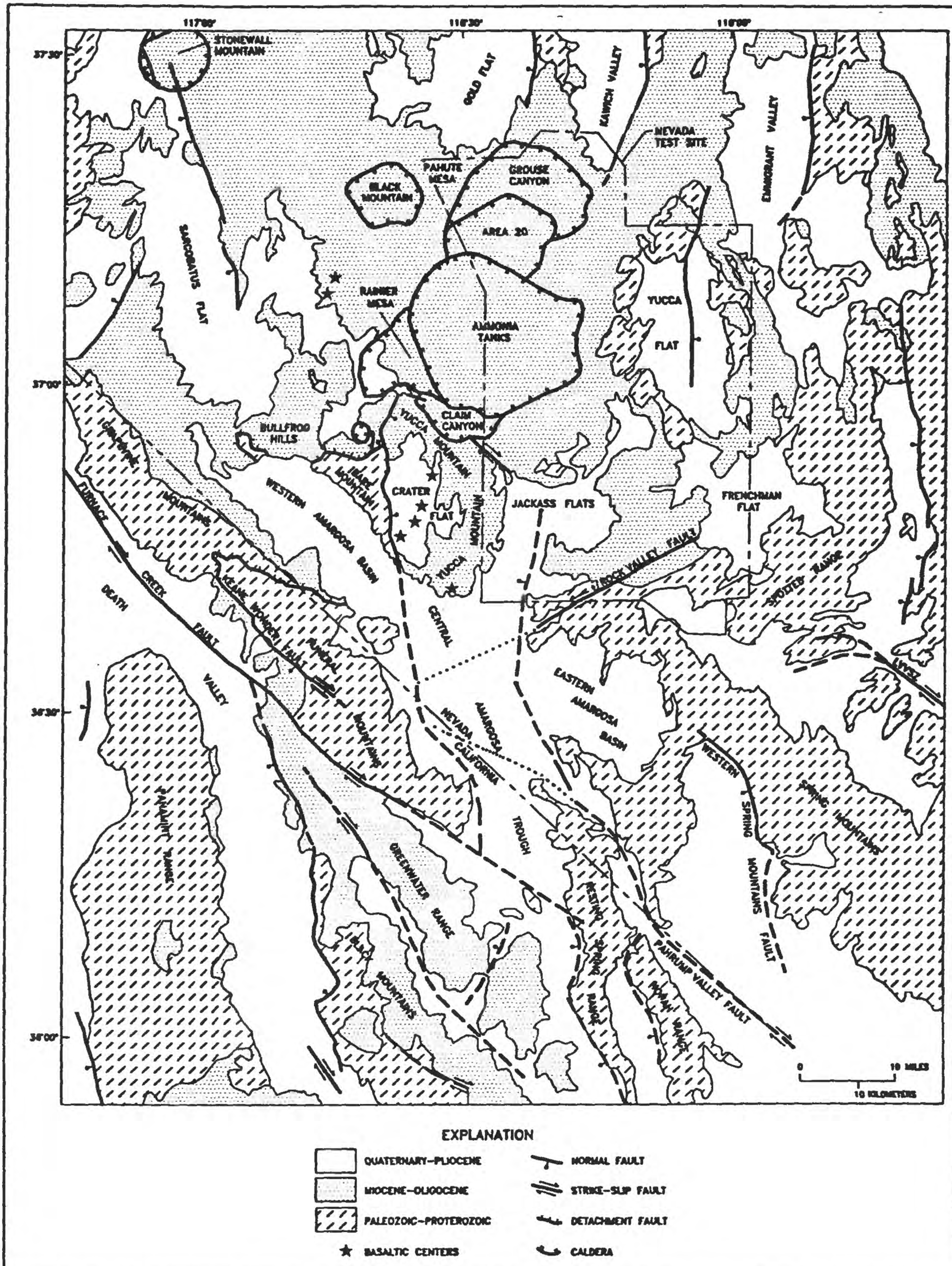

117°00'
116°30'
116°00'
37°30'
37°00'
36°30'
36°00'
STONEWALL MOUNTAIN
GOLD FLAT
KAWICH VALLEY
NEVADA TEST SITE
EMIGRANT VALLEY
PAHUTE MESA
BLACK MOUNTAIN
GROUSE CANYON
AREA 20
SARCOBATUS FLAT
RAINIER MESA
AMMONIA TANKS
YUCCA FLAT
CLAIM CANYON
BULLFROG HILLS
YUCCA MOUNTAIN
BARE MOUNTAIN
CRATER FLAT
JACKASS FLATS
FRENCHMAN FLAT
WESTERN AMARGOSA BASIN
ROCK VALLEY FAULT
SPOTTED RANGE
DEATH VALLEY
FURNACE CREEK FAULT
KEANE WONDER FAULT
FUNERAL MOUNTAINS
CENTRAL
EASTERN AMARGOSA BASIN
LVVSZ
NEVADA CALIFORNIA
AMARGOSA TROUGH
WESTERN SPRING MOUNTAINS
SPRING MOUNTAINS FAULT
PANAMINT RANGE
GREENWATER RANGE
RESTING SPRING RANGE
PAHRUMP VALLEY FAULT
NOPAH RANGE
BLACK MOUNTAINS
0
10 MILES
10 KILOMETERS
EXPLANATION
QUATERNARY-PLIOCENE
MIOCENE-OLIGOCENE
PALEOZOIC-PROTEROZOIC
BASALTIC CENTERS
NORMAL FAULT
STRIKE-SLIP FAULT
DETACHMENT FAULT
CALDERA

Figure 2

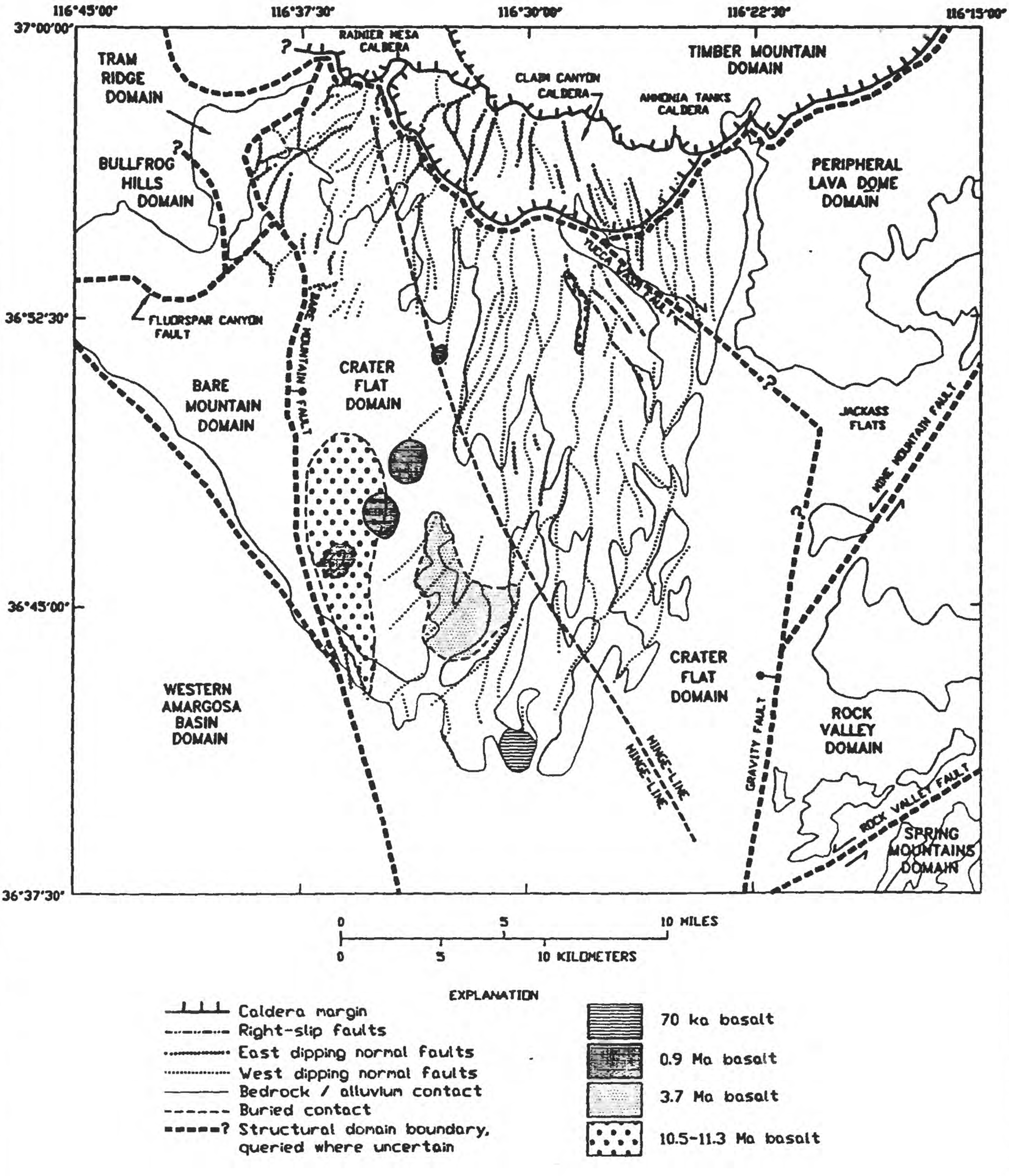
116°45'00"
116°37'30"
116°30'00"
116°22'30"
116°15'00"
37°00'00"
36°52'30"
36°45'00"
36°37'30"
RAINIER MESA CALDERA
CLAIM CANYON CALDERA
AMMONIA TANKS CALDERA
TIMBER MOUNTAIN DOMAIN
TRAM RIDGE DOMAIN
BULLFROG HILLS DOMAIN
PERIPHERAL LAVA DOME DOMAIN
YUCCA WASH FAULT
FLUORSPAR CANYON FAULT
BARE MOUNTAIN FAULT
BARE MOUNTAIN DOMAIN
CRATER FLAT DOMAIN
JACKASS FLATS
MINE MOUNTAIN FAULT
HINGE-LINE
WESTERN AMARGOSA BASIN DOMAIN
CRATER FLAT DOMAIN
GRAVITY FAULT
ROCK VALLEY DOMAIN
ROCK VALLEY FAULT
SPRING MOUNTAINS DOMAIN
0
5
10 MILES
0
5
10 KILOMETERS
EXPLANATION
Caldera margin
Right-slip faults
East dipping normal faults
West dipping normal faults
Bedrock / alluvium contact
Buried contact
Structural domain boundary, queried where uncertain
70 ka basalt
0.9 Ma basalt
3.7 Ma basalt
10.5-11.3 Ma basalt

Figure 3

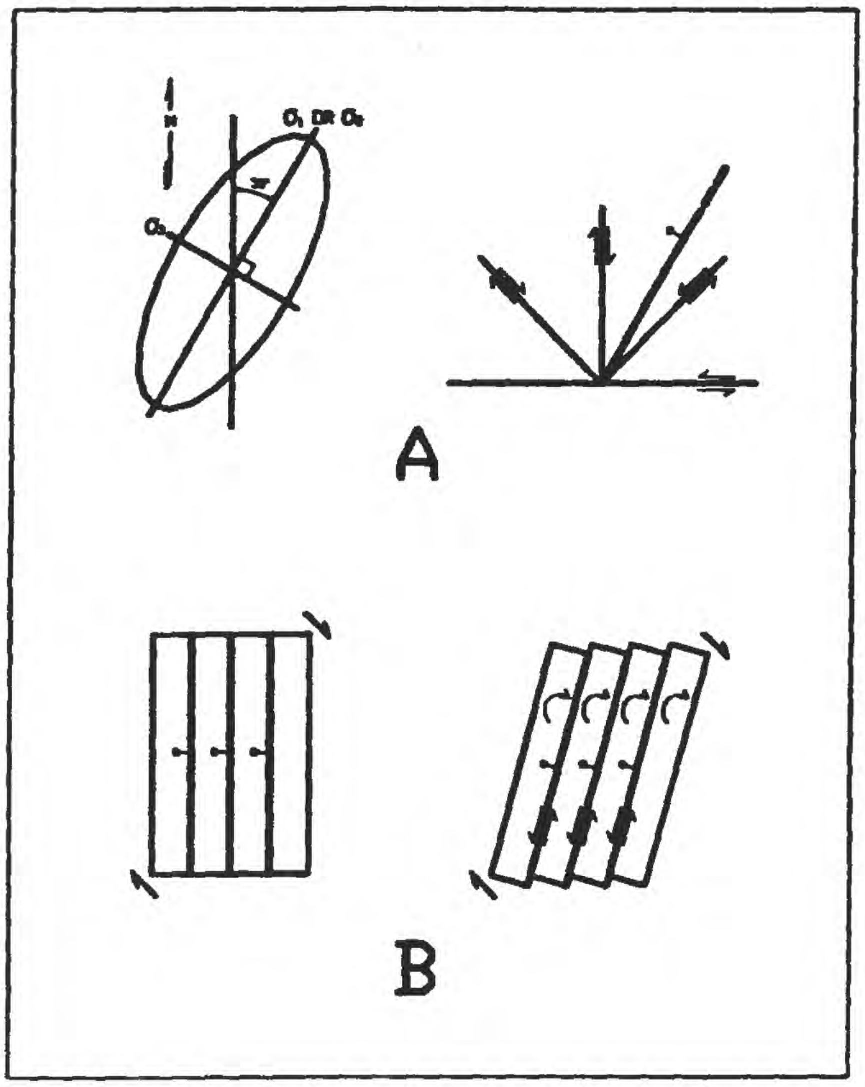

Figure 4

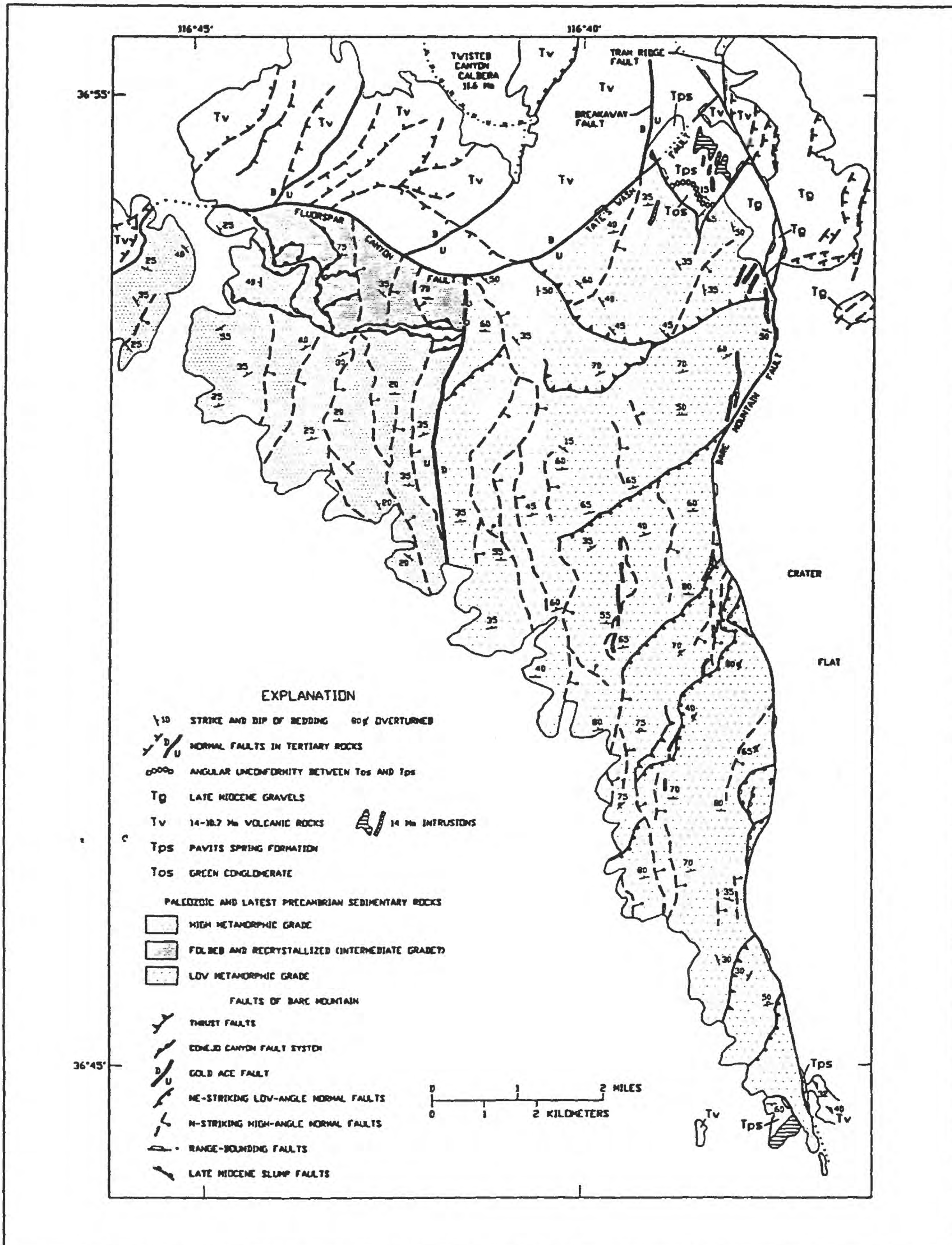
116°45'
116°40'
36°55'
36°45'
TWISTED CANYON CALDERA 11.6 Ma
TRAM RIDGE FAULT
BREAKAWAY FAULT
FLUORSPAR CANYON FAULT
TATE'S WASH
BARE MOUNTAIN FAULT
CRATER
FLAT
Tv
Tps
Tos
Tg
EXPLANATION
STRIKE AND DIP OF BEDDING
80 OVERTURNED
NORMAL FAULTS IN TERTIARY ROCKS
ANGULAR UNCONFORMITY BETWEEN Tos AND Tps
Tg LATE MIOCENE GRAVELS
Tv 14-10.7 Ma VOLCANIC ROCKS
14 Ma INTRUSIONS
Tps PAVITS SPRING FORMATION
Tos GREEN CONGLOMERATE
PALEOZOIC AND LATEST PRECAMBRIAN SEDIMENTARY ROCKS
HIGH METAMORPHIC GRADE
FOLDED AND RECRYSTALLIZED (INTERMEDIATE GRADE?)
LOW METAMORPHIC GRADE
FAULTS OF BARE MOUNTAIN
THRUST FAULTS
CONEJO CANYON FAULT SYSTEM
GOLD ACE FAULT
NE-STRIKING LOW-ANGLE NORMAL FAULTS
N-STRIKING HIGH-ANGLE NORMAL FAULTS
RANGE-BOUNDING FAULTS
LATE MIOCENE SLUMP FAULTS
0 1 2 MILES
0 1 2 KILOMETERS

Figure 5

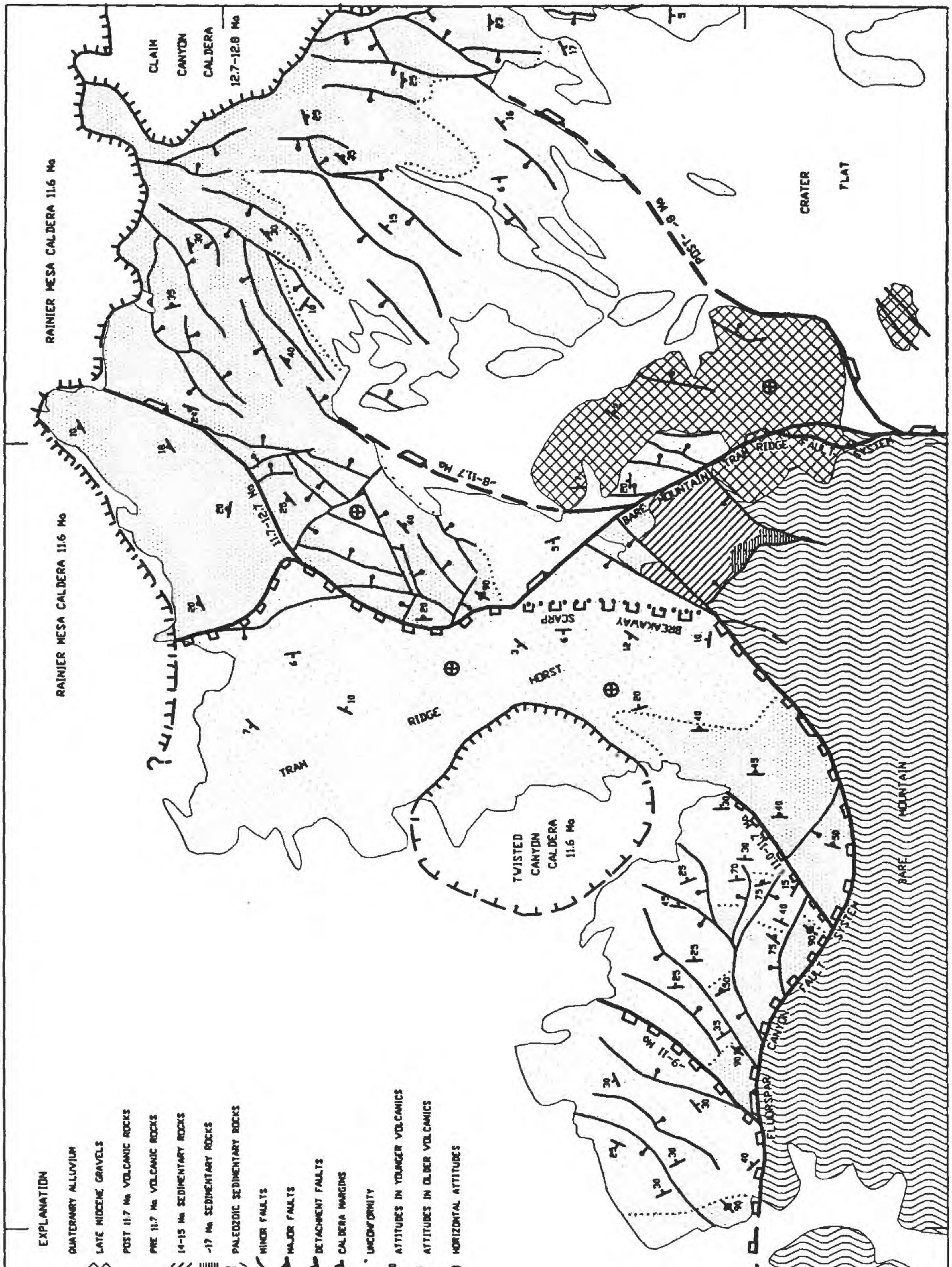
EXPLANATION
QUATERNARY ALLUVIUM
LATE MIOCENE GRAVELS
POST 11.7 Ma VOLCANIC ROCKS
PRE 11.7 Ma VOLCANIC ROCKS
14-15 Ma SEDIMENTARY ROCKS
~17 Ma SEDIMENTARY ROCKS
PALEOZOIC SEDIMENTARY ROCKS
MINOR FAULTS
MAJOR FAULTS
DETACHMENT FAULTS
CALDERA MARGINS
UNCONFORMITY
ATTITUDES IN YOUNGER VOLCANICS
ATTITUDES IN OLDER VOLCANICS
HORIZONTAL ATTITUDES
CLAIM CANYON CALDERA 12.7-12.8 Ma
RAINIER MESA CALDERA 11.6 Ma
RAINIER MESA CALDERA 11.6 Ma
CRATER FLAT
TWISTED CANYON CALDERA 11.6 Ma
TRAM RIDGE HORST
BREAKAWAY SCARP
BARE MOUNTAIN TRAM RIDGE FAULT SYSTEM
FLUORSPAR CANYON FAULT SYSTEM
BARE MOUNTAIN
3 MILES
3 KILOMETERS

FIGURE 6

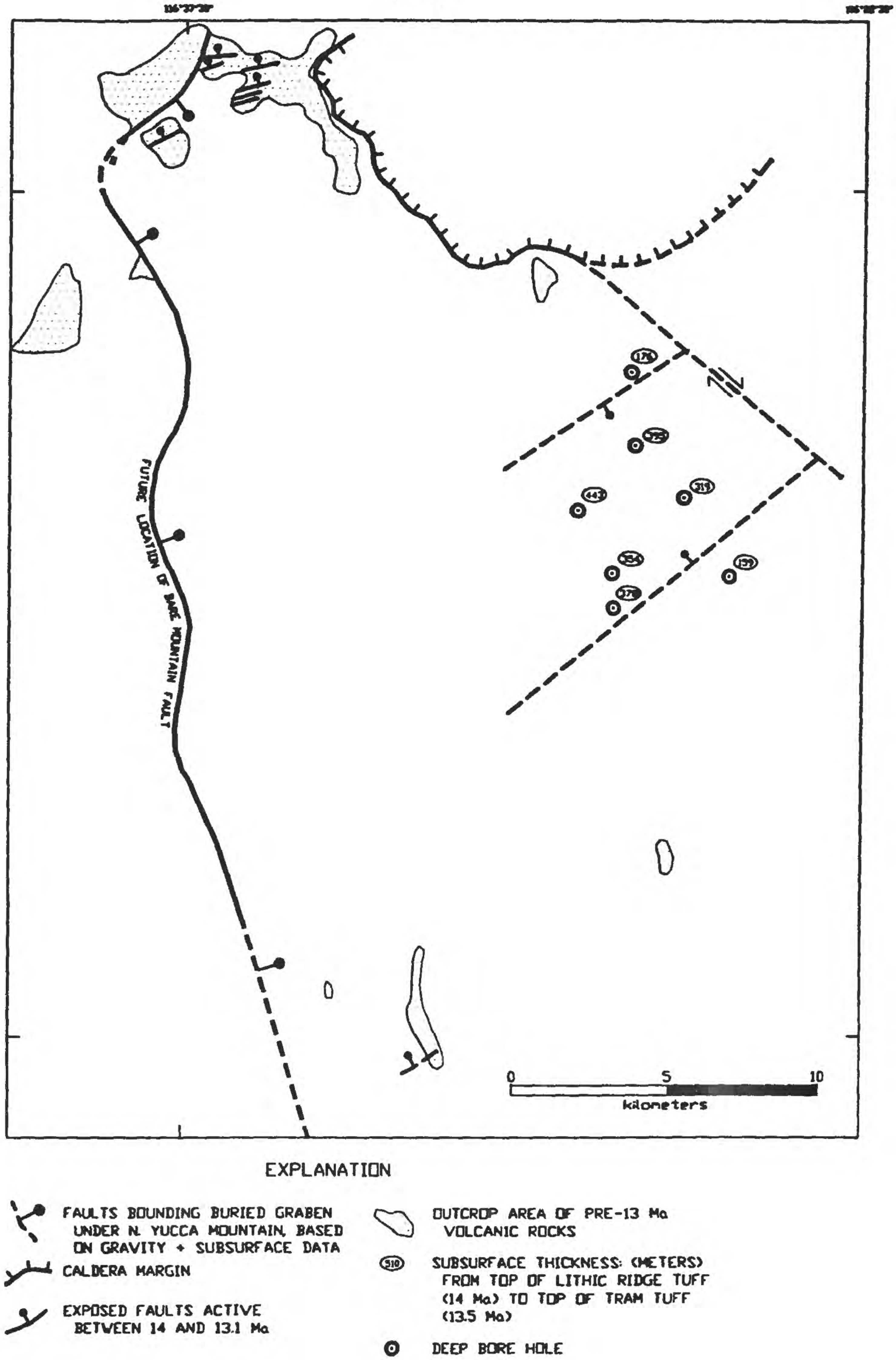
FUTURE LOCATION OF BARE MOUNTAIN FAULT
0
5
10
kilometers
EXPLANATION
FAULTS BOUNDING BURIED GRABEN UNDER N. YUCCA MOUNTAIN, BASED ON GRAVITY + SUBSURFACE DATA
CALDERA MARGIN
EXPOSED FAULTS ACTIVE BETWEEN 14 AND 13.1 Ma
OUTCROP AREA OF PRE-13 Ma VOLCANIC ROCKS
510
SUBSURFACE THICKNESS: (METERS) FROM TOP OF LITHIC RIDGE TUFF (14 Ma) TO TOP OF TRAM TUFF (13.5 Ma)
DEEP BORE HOLE

Figure 7

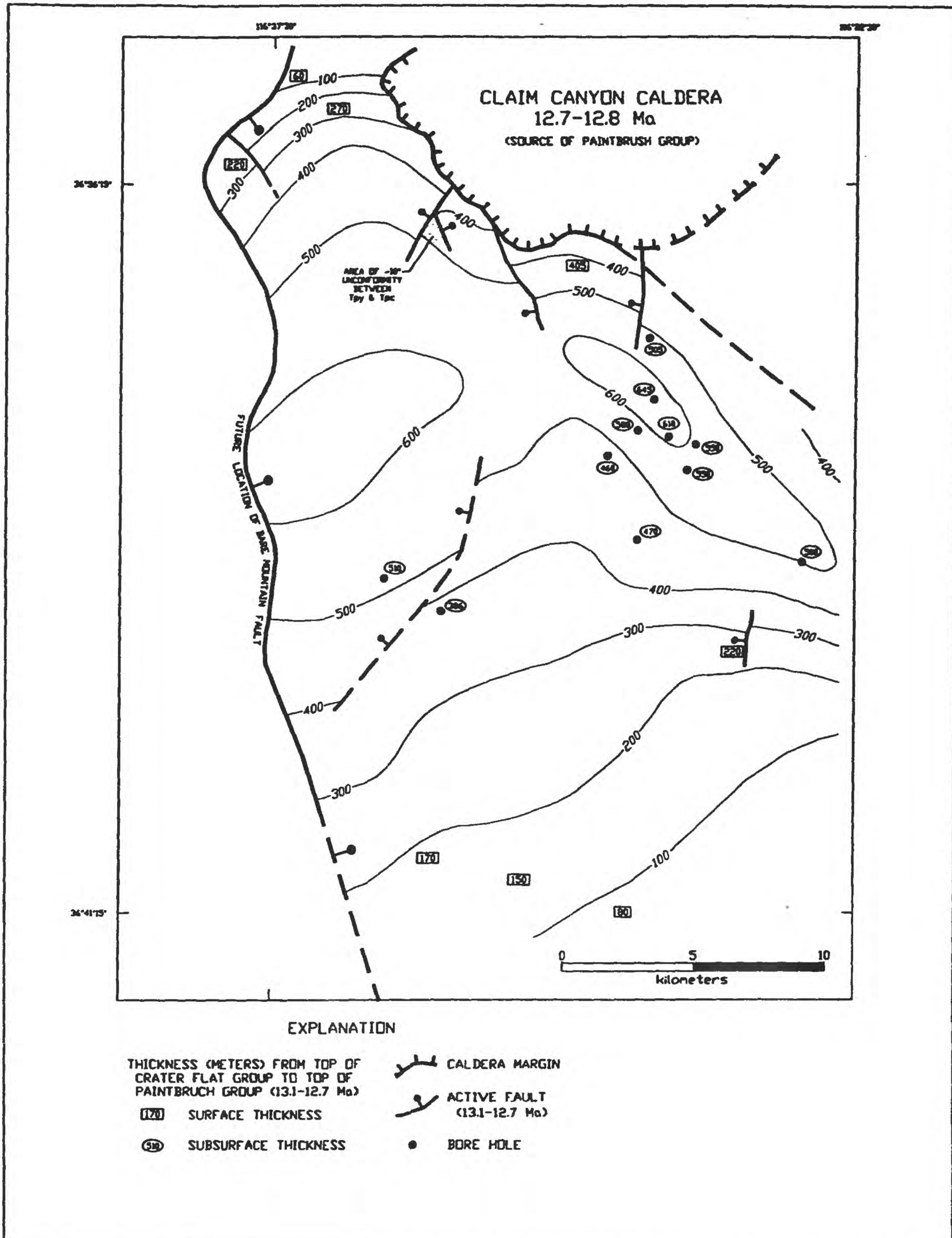
CLAIM CANYON CALDERA
12.7-12.8 Ma
(SOURCE OF PAINTBRUSH GROUP)
AREA OF ~10° UNCONFORMITY BETWEEN Tpy & Tpc
FUTURE LOCATION OF BARE MOUNTAIN FAULT
0
5
10
kilometers
EXPLANATION
THICKNESS (METERS) FROM TOP OF CRATER FLAT GROUP TO TOP OF PAINTBRUCH GROUP (13.1-12.7 Ma)
170 SURFACE THICKNESS
510 SUBSURFACE THICKNESS
CALDERA MARGIN
ACTIVE FAULT (13.1-12.7 Ma)
BORE HOLE

Figure 8

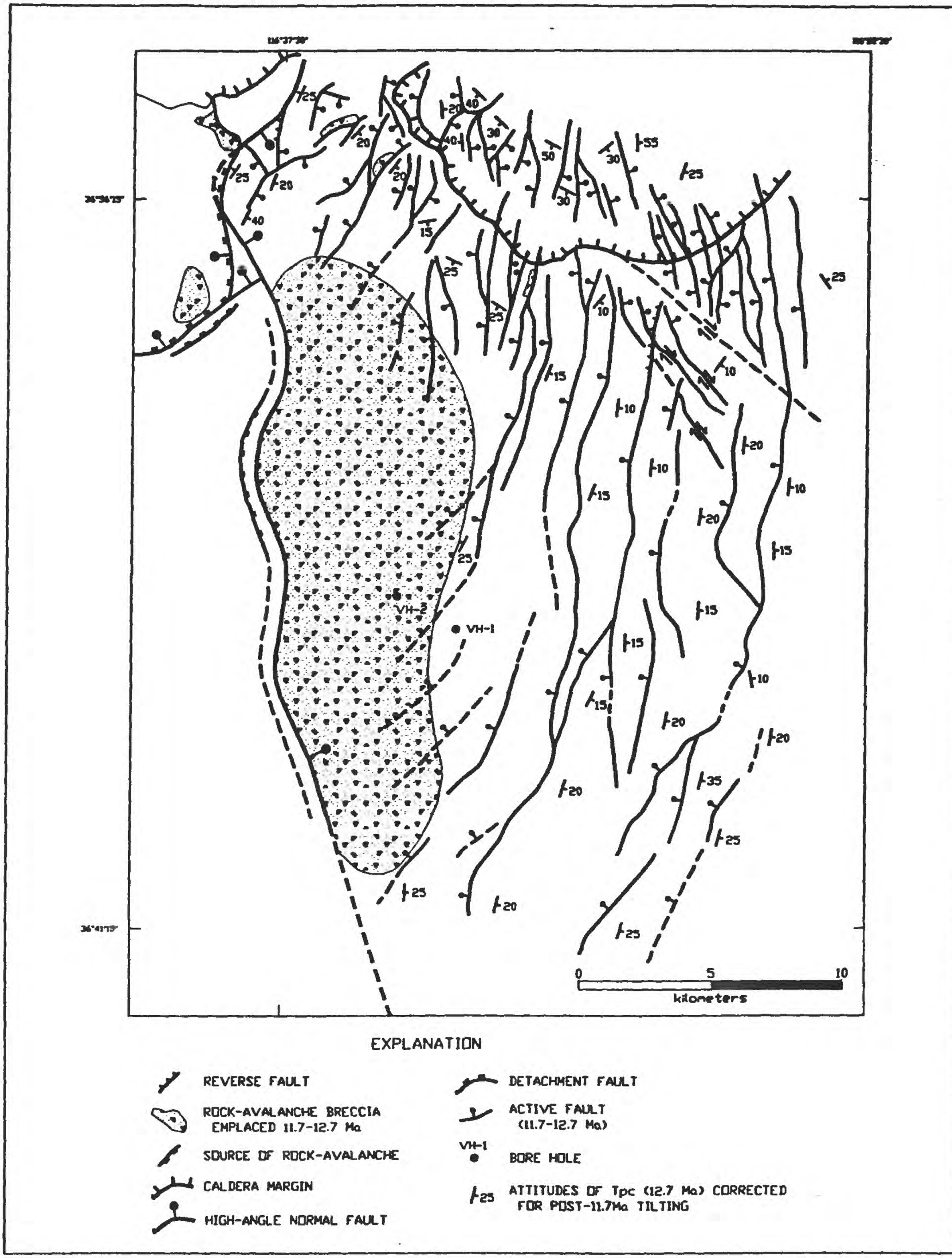
VH-2
VH-1
0
5
10
kilometers
EXPLANATION
REVERSE FAULT
ROCK-AVALANCHE BRECCIA EMPLACED 11.7-12.7 Ma
SOURCE OF ROCK-AVALANCHE
CALDERA MARGIN
HIGH-ANGLE NORMAL FAULT
DETACHMENT FAULT
ACTIVE FAULT (11.7-12.7 Ma)
VH-1
BORE HOLE
25
ATTITUDES OF Tpc (12.7 Ma) CORRECTED FOR POST-11.7Ma TILTING

Figure 9

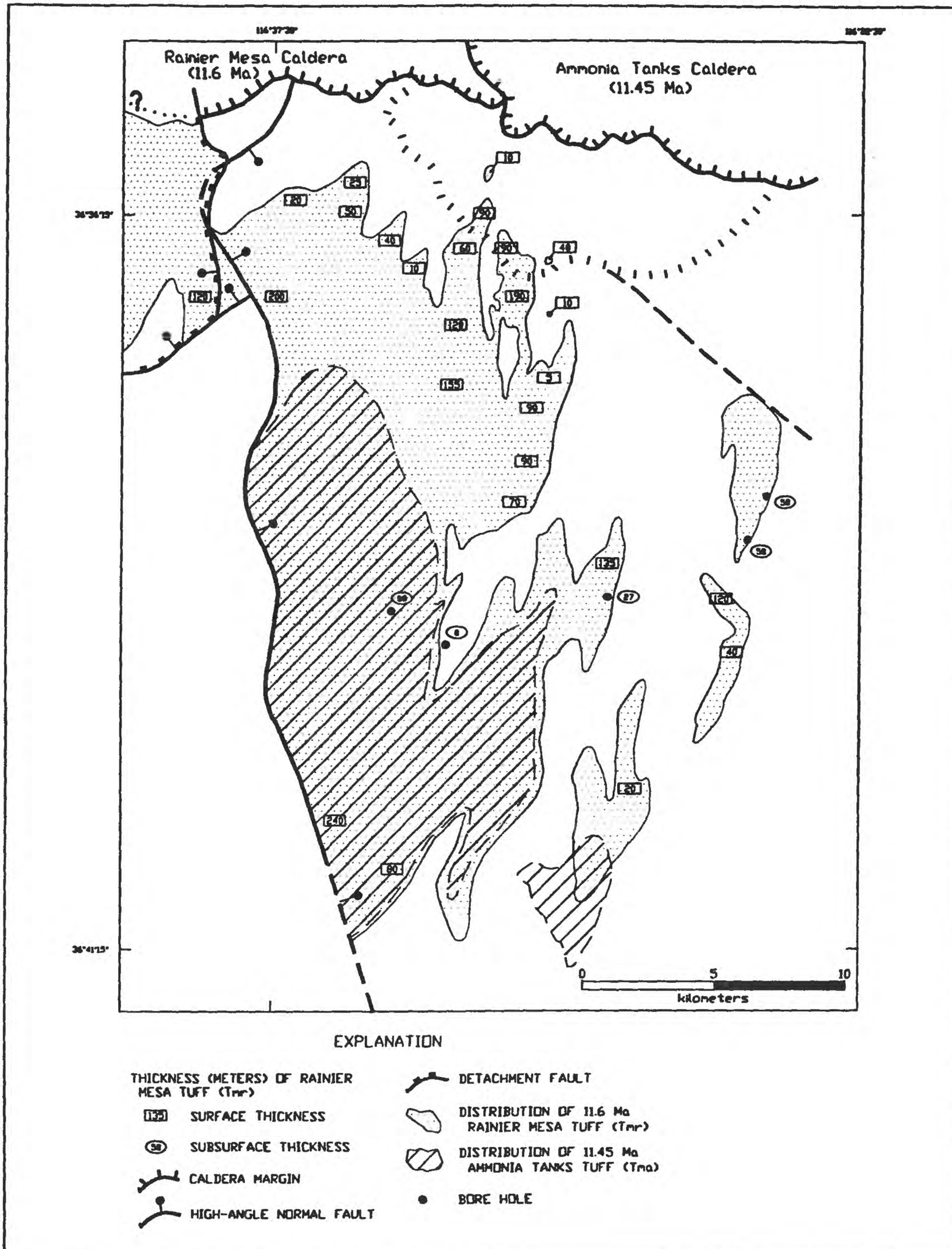
Rainier Mesa Caldera
(11.6 Ma)
Ammonia Tanks Caldera
(11.45 Ma)
0
5
10
kilometers
EXPLANATION
THICKNESS (METERS) OF RAINIER MESA TUFF (Tmr)
SURFACE THICKNESS
SUBSURFACE THICKNESS
CALDERA MARGIN
HIGH-ANGLE NORMAL FAULT
DETACHMENT FAULT
DISTRIBUTION OF 11.6 Ma RAINIER MESA TUFF (Tmr)
DISTRIBUTION OF 11.45 Ma AMMONIA TANKS TUFF (Tma)
BORE HOLE

Figure 10

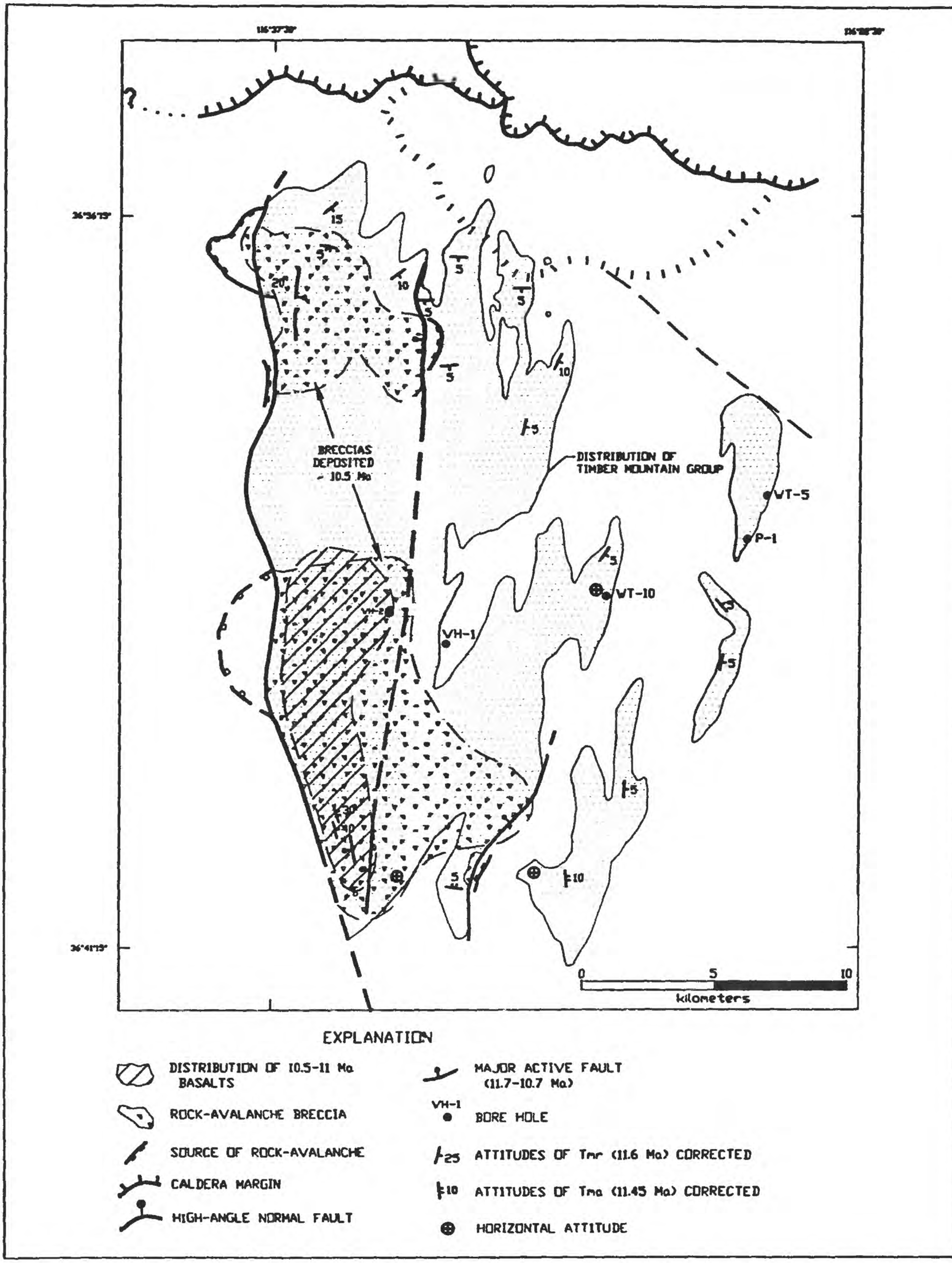
BRECCIAS
DEPOSITED
~10.5 Ma
DISTRIBUTION OF
TIMBER MOUNTAIN GROUP
WT-5
P-1
WT-10
VH-1
VH-2
0
5
10
kilometers
EXPLANATION
DISTRIBUTION OF 10.5-11 Ma
BASALTS
ROCK-AVALANCHE BRECCIA
SOURCE OF ROCK-AVALANCHE
CALDERA MARGIN
HIGH-ANGLE NORMAL FAULT
MAJOR ACTIVE FAULT
(11.7-10.7 Ma)
VH-1
BORE HOLE
25
ATTITUDES OF Tmr (11.6 Ma) CORRECTED
10
ATTITUDES OF Tma (11.45 Ma) CORRECTED
HORIZONTAL ATTITUDE

Figure 11

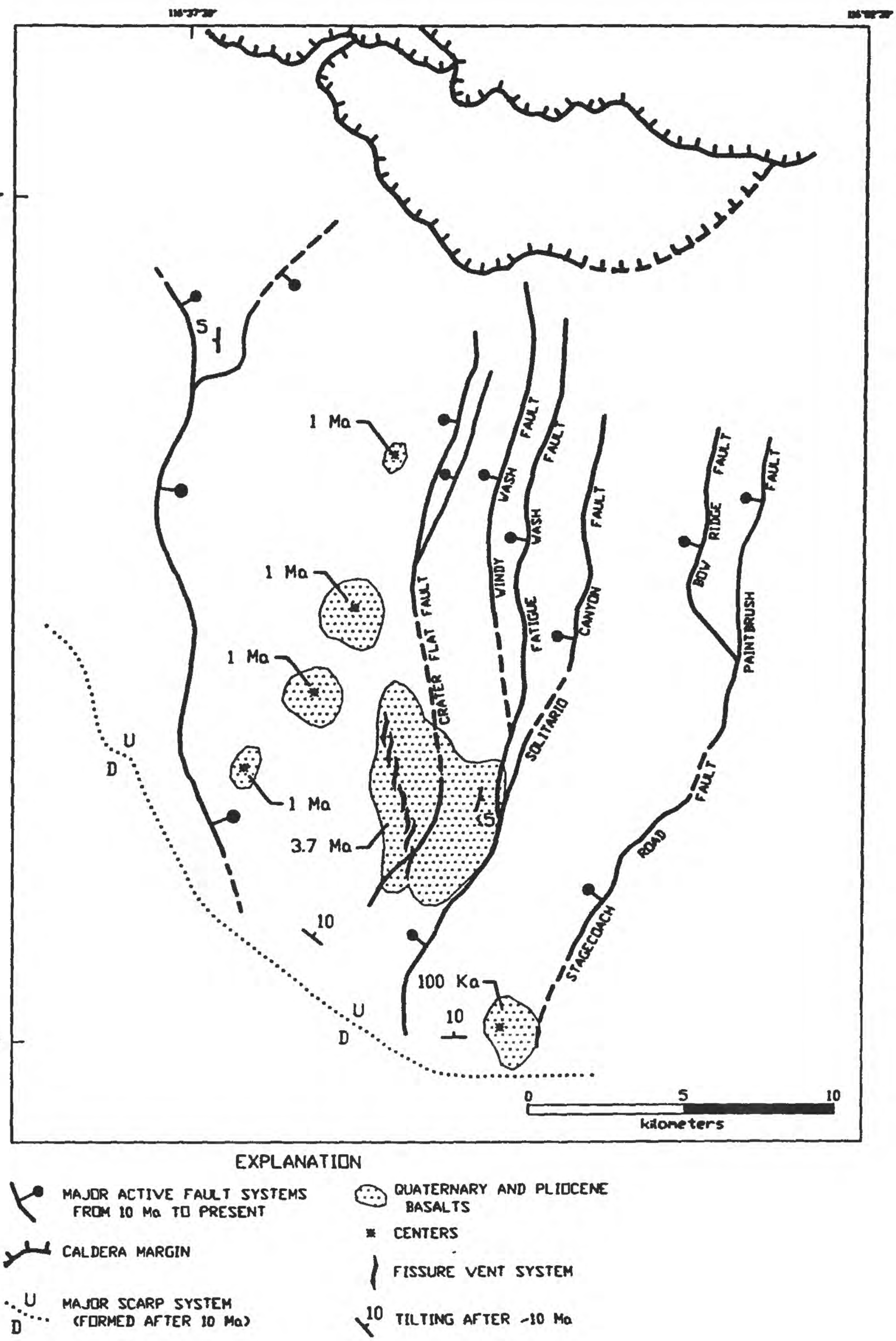
5
1 Ma
1 Ma
1 Ma
1 Ma
3.7 Ma
100 Ka
U
D
U
D
10
10
S
CRATER FLAT FAULT
WINDY WASH FAULT
FATIGUE WASH FAULT
SOLITARIO CANYON FAULT
BOW RIDGE FAULT
PAINTBRUSH FAULT
STAGECOACH ROAD FAULT
0
5
10
kilometers
EXPLANATION
MAJOR ACTIVE FAULT SYSTEMS FROM 10 Ma TO PRESENT
CALDERA MARGIN
U
D
MAJOR SCARP SYSTEM (FORMED AFTER 10 Ma)
QUATERNARY AND PLIOCENE BASALTS
CENTERS
FISSURE VENT SYSTEM
10
TILTING AFTER ~10 Ma

Figure 12

TABLE 1. AGES[1] AND GEOGRAPHIC EXTENTS OF THE VOLCANIC UNITS OF CRATER FLAT AND VICINITY AND STRATIGRAPHIC POSITIONS OF UNCONFORMITIES

Unit	Age (Ma)	Extent: Exposed area	Extent: Location	Unconformities
Pliocene and Quaternary volcanics:				
(interbedded with recent alluvium)				
Lathrop Wells cone	0.07	small	southeast Crater Flat only	
Bishop Tuff ashfall	0.7	small	widely scattered	
Crater Flat cinder cones	0.8	small	west Crater Flat only	
older Crater Flat flows	3.7	moderate	south Crater Flat only	
Latest Miocene units:				
Late Miocene basin fill	(10-5)	moderate	widespread in subsurface	
(locally includes:)				
Spearhead Tuff	7.5	small	north of Crater Flat only	
Unnamed ashfalls	8.5-7.6	small	widely scattered	
Unnamed related lavas	" "	large	west Bullfrog Hills/ Grapevine Mtns only	
Thirsty Canyon Tuff	9.4	small	north of Crater Flat only	
Basalts of Jackass Flats	10.5-9.5	moderate	Jackass Flats only	
Donavan Mountain Latite	10.0	moderate	Bullfrog Hills only	
				small angle, Bullfrog Hills
Rocks of Rainbow Mountain	(10.4)	moderate	east Bullfrog Hills	
landslide breccia	(10.5)	moderate	west Crater Flat	
				W.CraterFlat/BullfrogHills
Basalts of west Crater Flat	11.3-10.5	small	west Crater Flat	
Basalts of Fluorspar Canyon	11.1	moderate	widely scattered	
Major Volcanic Period (11-14 Ma) units:				
Timber Mountain Group:				
Ammonia Tanks Tuff	11.45	large	widespread with gaps	
tuff of Twisted Canyon	11.6	small	Fluorspar Hills only	
Rainier Mesa Tuff	11.6	very large	widespread	
Rhyo of Fluorspar Canyon	11.6-11.7	very large	widespread	
rock-avalanche breccia	12.6-11.7	numerous small	widespread	large, widespread
Windy Wash lavas/tuffs	12.5	moderate	north Crater Flat only	
Paintbrush Group:				
Tiva Canyon Tuff	12.7	very large	widespread	
				very local near calders
Yucca Mtn Tuff	12.7	moderate	north Crater Flat only	
Pah Canyon Tuff	12.8	small	north Crater Flat only	
Topopah Spring Tuff	12.8	large	widespread	
Calico Hills Formation tuffs	12.9	moderate	north Crater Flat only	
Crater Flat Group:				
Prow Pass Tuff	13.1	small	east Crater Flat only	buried fault scarps
Bullfrog Tuff	13.25	moderate	widespread in subsurface	
Prospector Pass Rhyolite	13.35	moderate	north Crater Flat only	
Tram Tuff	13.45	moderate	widespread in subsurface	
				local, northwest Crater Flat
Lithic Ridge Tuff	13.9	very small	widespread in subsurface	
older tuffs	~14	very small	widespread in subsurface	
				a disconformity at least
Pre-southwest Nevada volcanic field units:				
Pavits Spring Formation	(14-15.1)	small scattered	widespread in subsurface?	
				large angle, widespread?
oldest thick welded tuffs	(17-14.5)	small scattered	widespread in subsurface?	
green conglomerate	(17+?)	very small	widespread in subsurface?	
Pre-Tertiary units:				
Paleozoic/L. Proterozoic sedimentary rocks	PCZ-Dev	large	widespread in subsurface	

[1] Ages include $^{40}Ar/^{39}Ar$ determinations from Sawyer and others (1994) and Crowe and others (1995), and K-Ar determinations from Monsen and others (1992); ages in parentheses are poorly limited estimates.